Courseware Development for a Laboratory Class in Power Electronics

by

Mariano Alvira

Submitted to the Department of Electrical Engineering and Computer Science in partial fulfillment of the requirements for the degree of

Master of Engineering

at the

MASSACHUSETTS INSTITUTE OF TECHNOLOGY

[September 2005]
June 2005

Author ....
Department of Electrical Engineering and Computer Science
June 1, 2005

Certified by ....
Steven B. Leeb
Associate Professor
Thesis Supervisor

Accepted by ....
Arthur C. Smith
Chairman, Department Committee on Graduate Theses

Courseware Development for a Laboratory Class in Power Electronics

by

Mariano Alvira

Submitted to the Department of Electrical Engineering and Computer Science
on June 1, 2005, in partial fulfillment of the
requirements for the degree of
Master of Engineering

Abstract

This thesis introduces a new lab kit that is uniquely suited to teach power electronics: the Power NerdKit. The Power NerdKit is a self-contained prototyping system, which is easily incorporated into other systems such as an electric go-kart. Central to the kit is the card-rack prototyping area, where circuitry on PCB cards can be installed, interconnected, and tested. We present three prototyping PCB cards for use with the kit. Each of the cards has a common interconnection interface: up to five high current connections can be made via terminal lugs, and up to 26 low current connections can be made via card-edge connector. The first card provides solderless breadboard for constructing circuits and can connect with other cards through the standard interface. The second card is similar to the first, but is designed for circuits that must be soldered together. The last card, called the TriTotemII, implements three "totem-pole" circuits, which form the foundation of the converter topologies taught in the class. Finally the cards feature a unique method to attach oddly shaped devices using Unplated Through-hole Anchor Points. The lab exercises emphasize design. In Lab 1, the student: learns why switching circuits are useful; learns a few necessary control circuits; and builds a switching audio amplifier. In Lab 2, the student constructs a 1500W buck converter that drives an electric go-kart at variable speeds; they also design and build a 12W boosting power supply for a switching stereo amplifier of their construction. In Lab 3, the student designs and builds a high-voltage flyback converter and an electric fluorescent lamp ballast. Lastly, in Lab 4, the student explores how power electronics are used to drive induction and permanent magnet machines using a teaching motor specifically designed for this course.

Thesis Supervisor: Steven B. Leeb
Title: Associate Professor

Acknowledgements

Special thanks to those who made indispensable contributions to 6.131: Ariel Rodriguez for testing and realizing the control circuits taught in Lab 1 and used throughout 6.131; Candace Wilson for her excellent revisions of Lab 3; Eric Tung for his work on Lab 4; Rob Cox, Al-Thaddeus Avestruz, and Warit Wichakool for their teaching assistance; the students of 6.188 (6.131's initial course number); and to Professors James L. Kirtley and Steven B. Leeb for their guidance and support. And my warmest gratitude to those who contributed with their love and support: Mom, Dad, my sisters, and Issel; this would not have been possible without you.

This thesis was made possible by essential funding from The Cambridge-MIT Institute (CMI), with additional funding from the U.S. Navy Office of Naval Research, and the Grainger Foundation.

Contents

List of Figures

Chapter 1

Introduction

THE purpose of electrical engineering laboratory classes at MIT is to teach students how to design and build circuits and systems. The MIT/EECS laboratory curriculum includes classes that cover many topics in electrical engineering and computer science, in a hands-on fashion, including analog circuits, digital circuits, microcontrollers, and bio-electrical systems. The topic of power electronics, however, was unrepresented, in part because the traditional laboratory prototyping tools are unsuitable to teach this subject. This thesis presents a new teaching system that is suitable for use in a power electronics laboratory. This system enabled MIT/EECS to offer the "Power Electronics Laboratory", 6.131, as part of the undergraduate curriculum. The teaching tools and labs described here are designed to be: 1) focused; so that the student spends most of his time on the aspects of the class that provide the most learning 2) affordable; so that the lessons can be taught with a reasonable budget and 3) maintainable; so that the class can be taught yearly.

Before 6.131, all EECS lab classes used the same basic teaching systems. To build their circuits, students use solderless breadboard inside a suitcase-like lab kit. This prototyping method has low year-to-year operating costs since the breadboard and components are reusable. The circuits taught in 6.131 use higher voltages and/or currents than the circuits typically taught in other classes. The teaching system presented in this thesis makes it possible to safely build high-current and/or high-voltage circuits in the cost and time requirements of an undergraduate laboratory class.

Chapter 2, presents a new laboratory kit specifically design for 6.131. The kit is a portable, self-contained, aluminum card-rack with integrated power supplies, batteries, charger, forced-air cooling, and a small, solderless prototyping area. It has handles and captive screws that allow the kit to be easily removed and installed into other systems. In this way, projects can be developed on a controlled bench-top environment, tested, and then literally dropped into an external system.

Chapter 3, presents a set of printed circuit boards (PCBs) used in 6.131. Two of the PCBs are general purpose prototyping cards: one card consists of a solderless breadboard and screw terminal blocks; the other card has printed copper traces in a standard connection pattern. The third card, called the Tri-Totem II (TTII), is a fundamental building block of the circuits taught in 6.131. It provides a set of three totem poles and independent MOSFET drivers; it is possible to construct a wide range of power converters with this topology.

Chapters 4, 5, 6, 7, present the four lab exercises for the class. Chapter 4 presents Lab 1, where the student learns the control circuits that will be used throughout the course. Chapters 5 and 6 present Labs 2 and 3 respectively, where the student builds several different power converters — starting with the canonical cell buck and boost converters in Lab 2, and advanced topologies in Lab 3, such as the flyback, resonant, and phase-controlled converters. Chapter 7 presents Lab 4, where the student builds motor drive for a permanent magnet machine and a 3-phase induction machine.

Chapter 8, presents the design review and checkoff methods used to assess student progress, as well as student feedback from the initial course offering.

Chapter 2

The PowerNerd Kit

THE power circuits taught in 6.131 have to process higher currents and/or voltages than what is typically built in a teaching lab at MIT. For instance, in Lab 2, students build a circuit that drives an electric go-kart. This requires a circuit capable of delivering 30A surge currents. For applications such as the go-kart, many of the circuits have to be soldered together for them to work safely and reliably. The typical breadboard prototyping system would be inadequate for this class.

Typically in laboratory classes, each student is issued a "NerdKit", which is a suitcase-like prototyping kit. The most basic NerdKits provide sufficient space to build circuitry on solderless breadboard and also provide fixed voltage power supplies. Modern versions of the NerdKit have some basic test equipment built-in; the NerdKit used in 6.115, for example, has a signal generator, two push-buttons, a speaker, several throw switches, and a logic monitor, among its extra "bells-and-whistles". While portable, like a suitcase, the NerdKits are not self-contained: they need to be plugged into the wall outlet when used. The traditional NerdKit also does not support solder-based prototypes and can not be used to construct high power circuits.

The 6.131 laboratory kit needs to be portable and self-contained if students are to use it for exercises like constructing a go-kart drive. The kit must also provide safety while maintaining convenient access for testing, revealing a design challenge: to enhance safety, the circuit must be isolated from the student (preferably by encasing it in an electrically safe box) — but to enhance usability, exposed prototyping areas are preferred. The kit must also be inexpensive to manufacture and easily maintained so as not to strain academic budgets.

In the final prototyping system, printed circuit boards (PCBs) are used in a cardrack enclosure. This custom cardrack is the center piece of the new lab kit designed for 6.131 — the "Power

NerdKit".

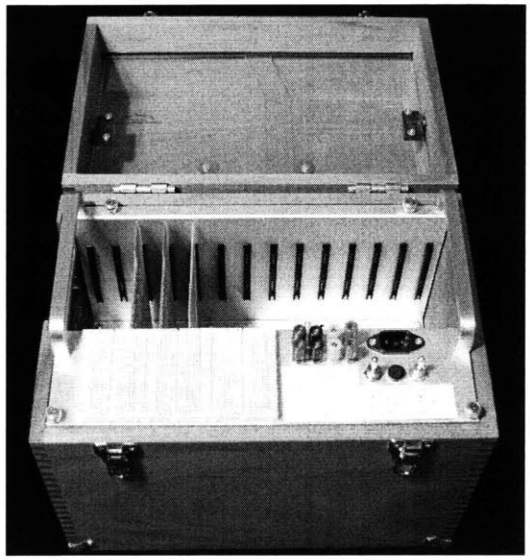

Figure 2.1: The Power-NerdKit inside its mahogany carrying case.

The Power NerdKit is shown in Figure 2.1 and Figure 2.2. In Figure 2.2, the kit has been removed from its carrying case and its main components are labeled. The main prototyping space of the lab kit is the cardrack. In here, cards are enclosed by aluminum on three sides, which protects the student. The bottom of the cardrack, shown in Figure 2.3, is vented and has a fan to cool the circuits in the rack. The front panel of the kit has a small, solderless prototyping area as well as electrical connections to the power compartment. The kit also has handles and captive thumb screws on its front face that allow the kit to be easily removed and installed into other systems. These features are illustrated in Figure 2.4.

The Power NerdKit chassis is constructed from two custom sheet metal parts: the power-cage and the card-cage. The manufacturing drawings for the power- and card-cage are included in Appendix A.2 and A.3, respectively. The power-cage is secured to the card-cage with eight nuts and bolts. Two washers on each bolt separate the cages; this provides a gap for the wires from the fan to go inside the power compartment, and to give clearance for the cardguides. Fourteen pairs of plastic cardguides line the inside of the card-cage producing the cardrack prototyping area. Two handles bridge and support the cardrack, and four captive thumb screws are snapped into its front face of the card-cage. Figure 2.5 shows a cardguide, captive screw, and handle used in the Power

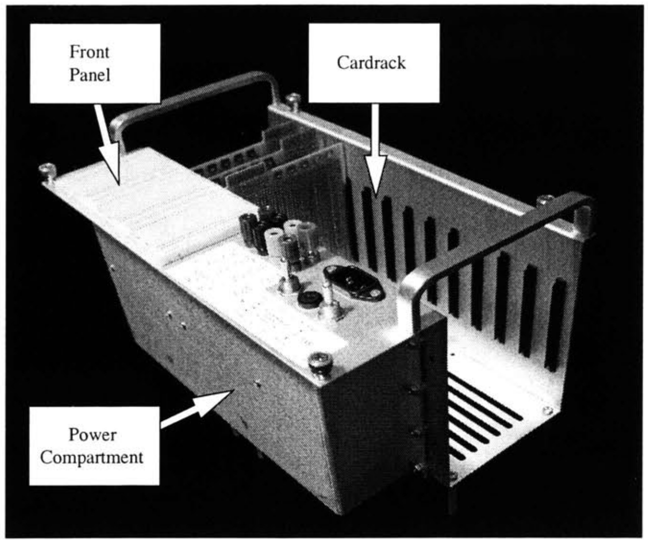

Figure 2.2: Components of the Power NerdKit

NerdKit.

The power compartment contains a dual +12V/-12V off-line supply, a +5V off-line supply, two 12V 4Ah lead-acid batteries, and a charger for the batteries. The inside of the power compartment is show in Figure 2.6 and the electrical connections are shown in Figure 2.7. The Main Power Supply (MPS) consists of a Mean-Well dual +12V/1A, -12V/1A supply and a Mean-Well single +5V/5A supply. These supplies have no minimum load requirement and have excellent short circuit protection. The Charging Power Supply (CPS) is a 30VDC, Class 2, line transformer plugged into a extension cord. The other end of the extension cord is stripped and connects to the supply switch (SW_{Supply}). The supply switch is a on-off-on SPDT, switch. It can turn either the MPS on, the CPS on, or both off. The AC line connects to the power compartment circuitry through a IEC connector on the front panel. It then passes through a fuse, and then to SW_{Supply}. The fuse is accessible on the front panel. Earth ground is connected to the Power NerdKit chassis and to a front panel banana plug. The output of the MPS (+5V, +12V, -12V and COM) are accessible via the banana plugs on the front panel. The batteries are connected in series, with the two ends and the center nodes provided on the front panel banana plugs. SW_{FAN} is an on-off-on SPDT switch that connects the fans to either, $+12V_{MPS}$, $-12V_{Batt}$, or turns them off.

Figure 2.8 shows the details of the interface to the power compartment. On the top right

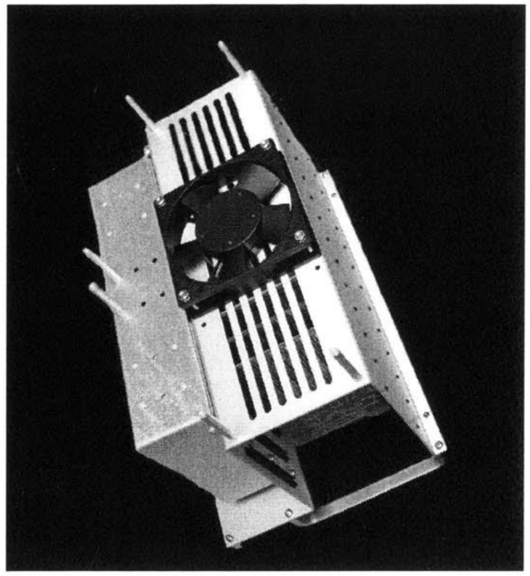

Figure 2.3: The underside of the Power NerdKit.

is the IEC connector to power the AC portions of the kit. The chassis is earth grounded *only* when the kit is plugged into the wall. The chassis is also connected to the green banana plug on the lower right. Figure 2.9 shows the front panel sticker explaining how to operate the kit. To charge the batteries in the kit, you flip the left switch down. To power the internal supplies you flip the left switch up. To run the fans from the internal supplies you flip the right switch up (the left switch must also be up). To run the fans from the batteries you flip the right switch down. For both switches, the middle position is off.

In the pilot production run, 163 kits were constructed for about $400 each, including assembly labor. The complete parts list and vendor information is included in Appendix A.

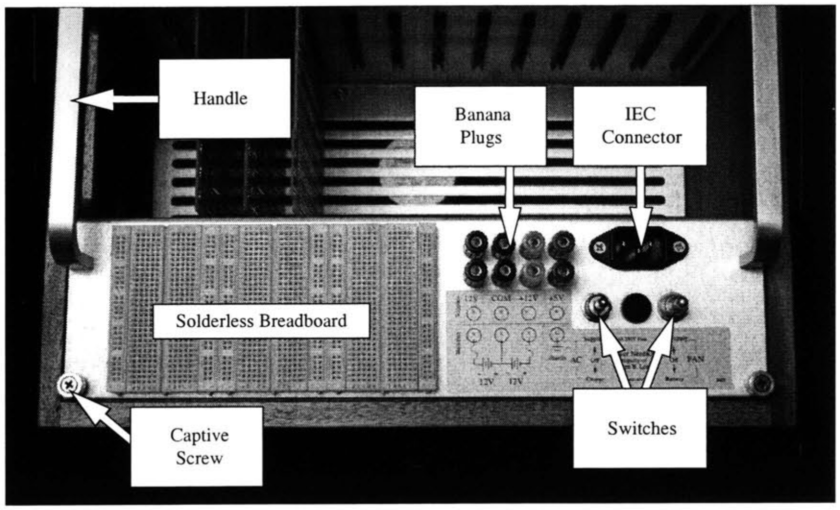

Figure 2.4: The front face of the Power NerdKit.

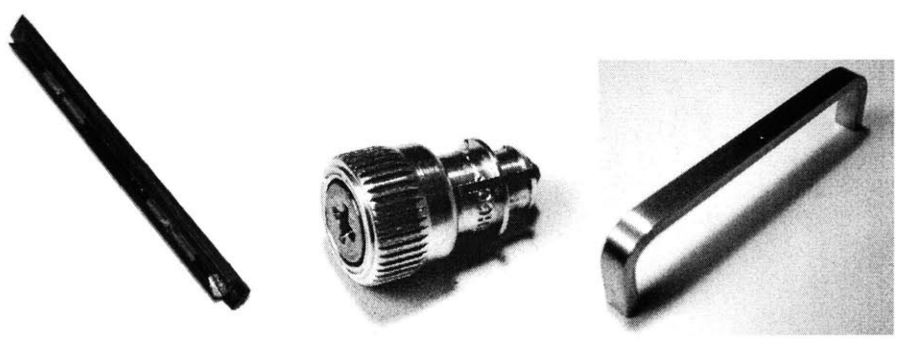

Figure 2.5: Left: Plastic cardguide used in the cardrack. Center: Handle. Right: Front panel captive screw.

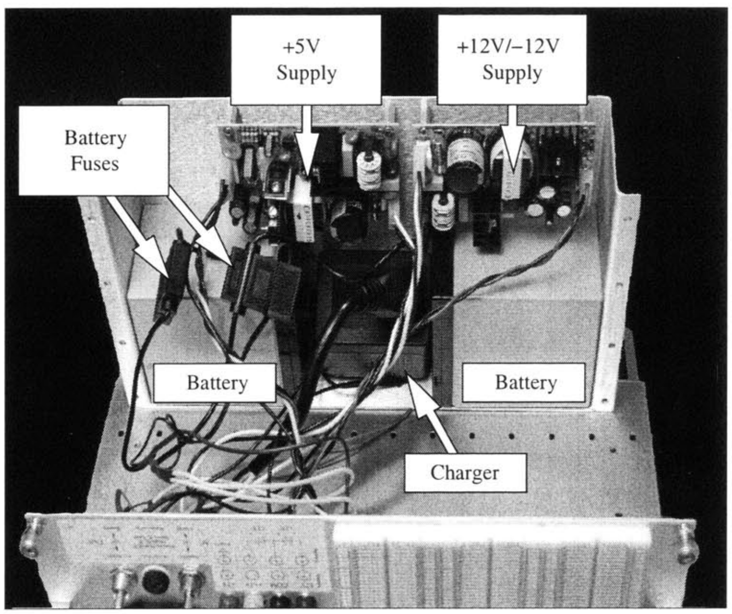

Figure 2.6: Inside the power compartment: on the top right are two Mean-Well power supplies that comprise the MPS; in the lower left and right are two 12V lead-acid batteries; in between the batteries is the wall-transformer that serves as the CPS. Also shown are the battery fuses.

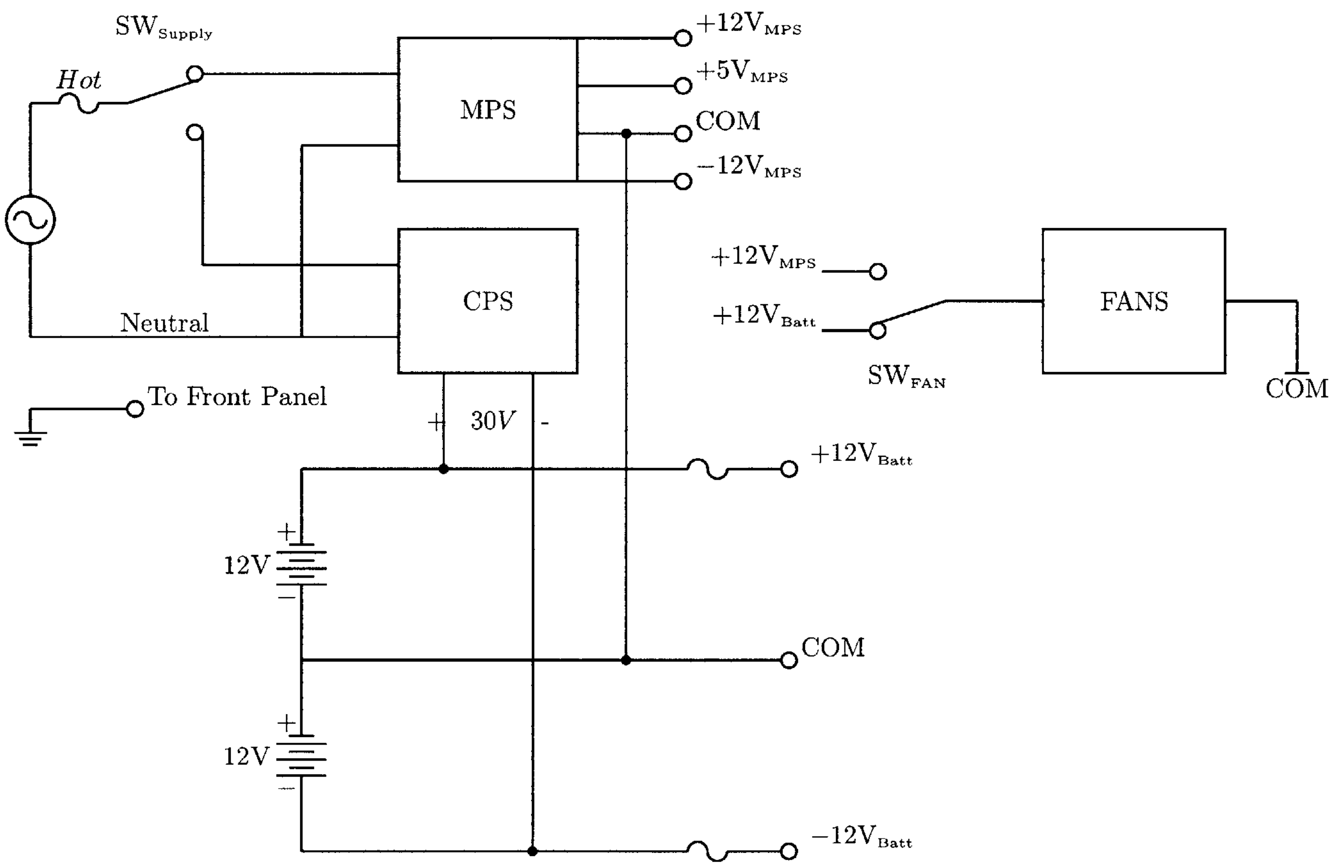

Figure 2.7: Power Compartment Circuit

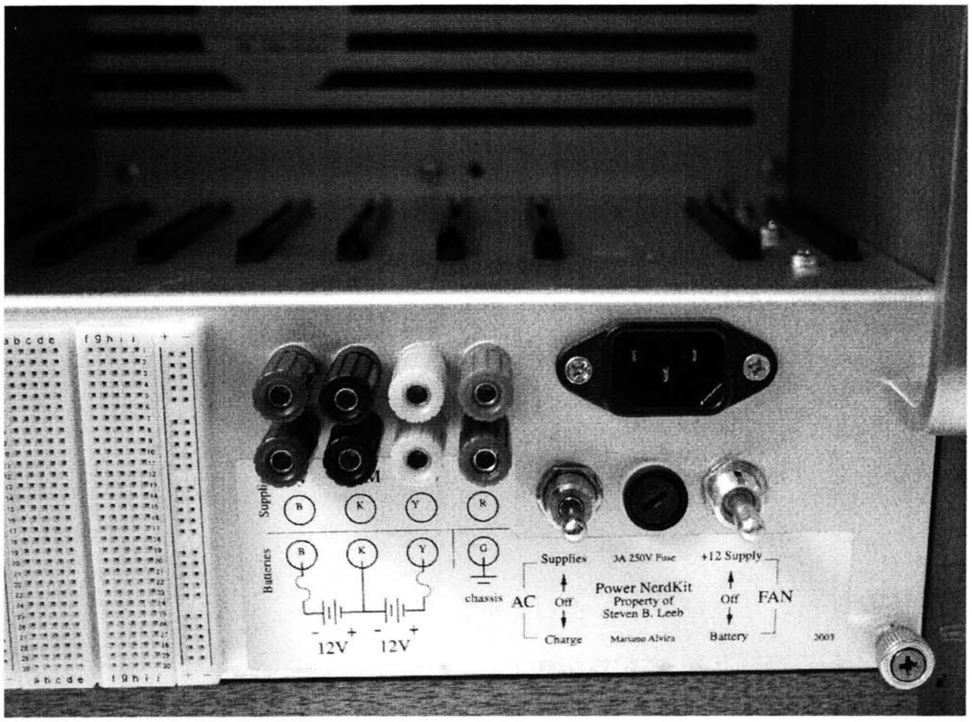

Figure 2.8: Power compartment interface.

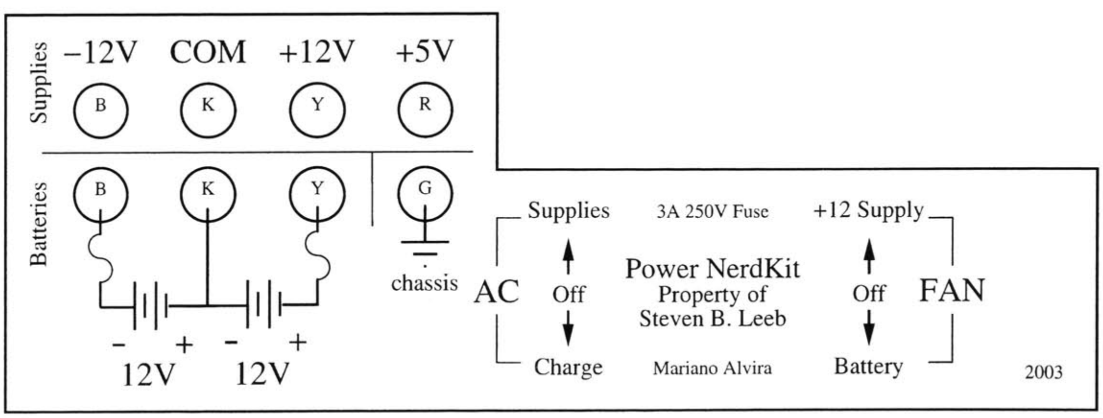

Figure 2.9: Front Panel Sticker.

Chapter 3

Three Prototyping PCBs

THREE PCBs have been designed to complete the 6.131 prototyping system. These cards, described in this Chapter, are: the Breadboard Card (BC), the Perfboard Solder Card (PSC), and the TriTotem II (TTII). Each of these cards feature the Common Power and Data Interface (CPDI), which provides a convenient mechanism for interconnecting multiple cards. The PSC and TTII also feature Unplated Through-hole Anchor Points (UTAPs), which provide a novel way to attach oddly shaped devices to the cards.

3.1 The Common Power and Data Interface

The CPDI provides a versatile and convenient method to distribute data and power across multiple cards. Each of the three 6.131 prototyping PCBs feature the CPDI, shown in Figure 3.1. The CPDI provides five power holes on the top-left side, and a card-edge connector with 26 contacts for low power signals on the top-right side.

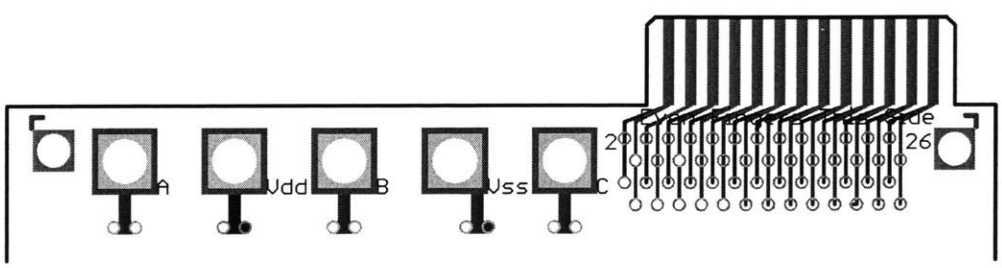

Figure 3.1: Power and Data Interface on the 6.131 prototyping PCBs.

Figure 3.2 shows how the CPDI is used to interconnect multiple cards. The three-tap card-edge cables, shown in Figure 3.3, are constructed by Digikey from 26-pin card-edge connectors from

CW Industries (Digikey: CCE26T-ND) and flat ribbon cable from 3M (Digikey: MC26M-X-ND; where X is the number of feet per roll and equals: {5, 10, 25, 50, 100, 300}).

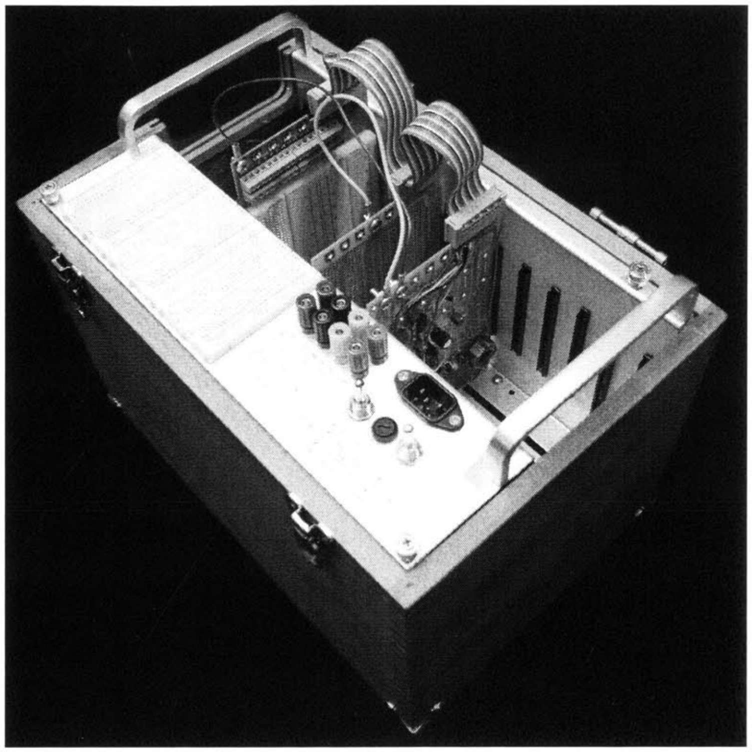

Figure 3.2: Three interconnected prototyping cards.

Figure 3.4 shows a close-up view of the power interconnections. Forked (Digikey: 920022-16-ND) or circular (Digikey: 920010-03-ND) terminal lugs are crimped to the ends of wire and secured to the power holes with a #10 nuts and bolts.

3.2 Unplated Through-hole Anchor Points

Often, oddly shaped devices must be used. For instance, in Lab 3 of 6.131, the students mount a fluorescent lamp onto a card, and then build an electronic ballast to drive the lamp. Inductors are another common component that can be challenging to secure to the cards. UTAPs are an innovative solution to this problem that do not require special connectors for each different device.

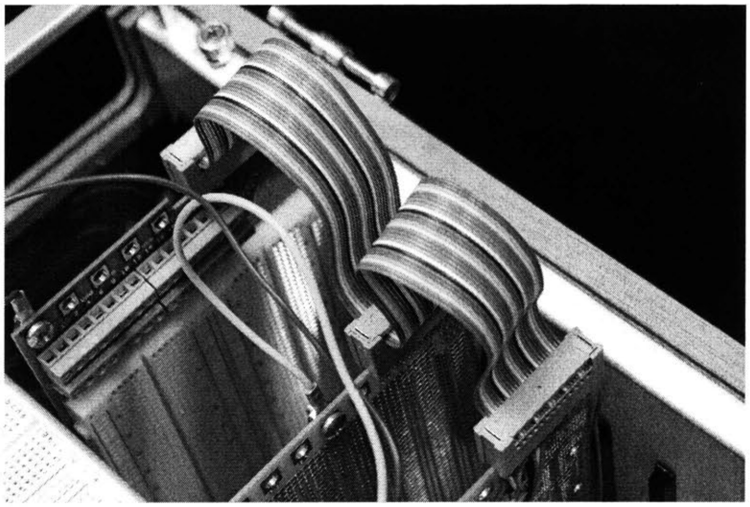

Figure 3.3: Close-up view of the data interconnections.

To create the anchor points, 0.1" dia. unplated through-holes were added between the horizontal traces. Figure 3.5 shows this arrangement on the prototyping area of the TTII card. The use of unplated through-holes preserves the solderless breadboard style of connection pattern. Figure 3.6 shows a typical example of how UTAPs are used. In this example, an inductor is secured to a TTII card with a pair of wire-ties through a set of UTAPs.

3.3 The Breadboard Card

The Breadboard Card (BC) is used to interface low power circuits to circuits on other cards. The BC is shown in Figure 3.7. The CPDI on the BC has been modified to provide room for a block of screw terminals: the five power terminals have been moved up and to the left, and a clearance notch for the card-edge connector has been added. The addition of the notch allowed us to increase the vertical dimension of the card. As a result, this board is the maximum vertical size that fits in the Power NerdKit. The two rows of screw terminal blocks give access to the signals on the card-edge connector and to each of the five power holes. Hook-up wire can be used to connect the CPDI to traces on the breadboard.

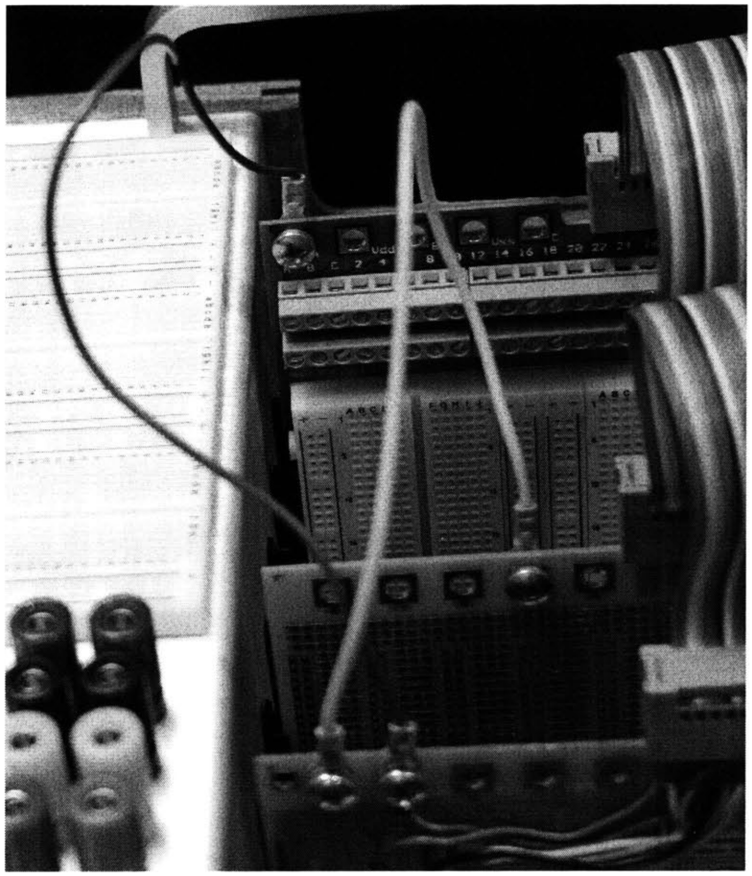

Figure 3.4: Close-up view of the power interconnections.

3.4 The Perfboard Solder Card

The PSC provides another method for the student to prototype circuits. While the BC is suitable for low-power circuitry, the PSC is suitable for high-power circuitry. The PSC is shown in Figure 3.8, its connection pattern is similar to the BC. The left-side of the prototyping area has UTAPs, and the top portion of the card has the standard 6.131 CPDI.

3.5 The TriTotem II

The final card, the Tri-Totem II, is the fundamental teaching tool used in 6.131. Many of the circuits in power electronics can be implemented with a circuit called a "Totem-Pole", shown in

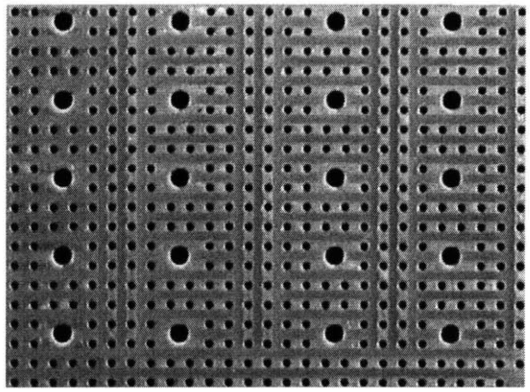

Figure 3.5: Unplated Through-hole Anchor Points on the TTII prototyping area.

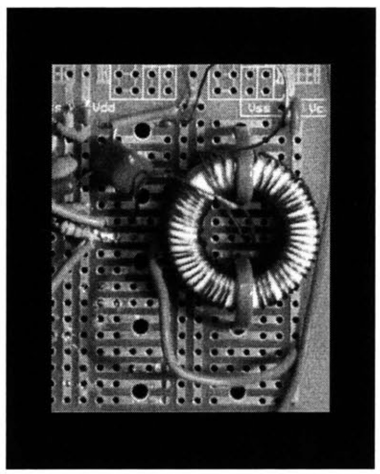

Figure 3.6: An inductor secured to a with wire-ties to a TTII through a set of UTAPs.

Figure 3.9. With one of these, versatile, and powerful circuits, students can make a buck-converter, boost-converter, buck/boost-converter, flyback or forward converter; with two, an H-Bridge; with three, a three-phase motor drive. The TTII is used in 6.131 to teach all of these applications.

The TTII provides a pre-laid set of three-totem poles with independent MOSFET drivers. The TTII can accommodate heatsinks (Digikey: HS225-ND) rated for $\frac{10^{\circ}\mathrm{C}}{\mathrm{W}}$ on each of the six MOSFETS. The power traces on the TTII are qualified to carry 15 Amps without reinforcement wires and up to 35 Amps with reinforcement wires. The TTII is also functional for applications that use up to 400V. Ample ground plane and tight layout controls parasitics which allows for fast switching. In Lab 2, for instance, students build power converts that switch at 250 kHz, and faster switching frequencies are possible with care.

The TTII is shown in Figure 3.10, and its full schematic is shown in Figure 3.11. As a prototyping aid, students are provided with laminated printouts that show the top and bottom layers of the TTII and PSC. The students use dry erase markers on these laminated sheets to plan their circuitry before they proceed to build it. During the term, 6.131 students are required to show the staff their layout plan before they can receive the parts needed to build their circuit. Small versions of these sheets are shown in Figure 3.12. Appendix B includes the full-sized versions of each.

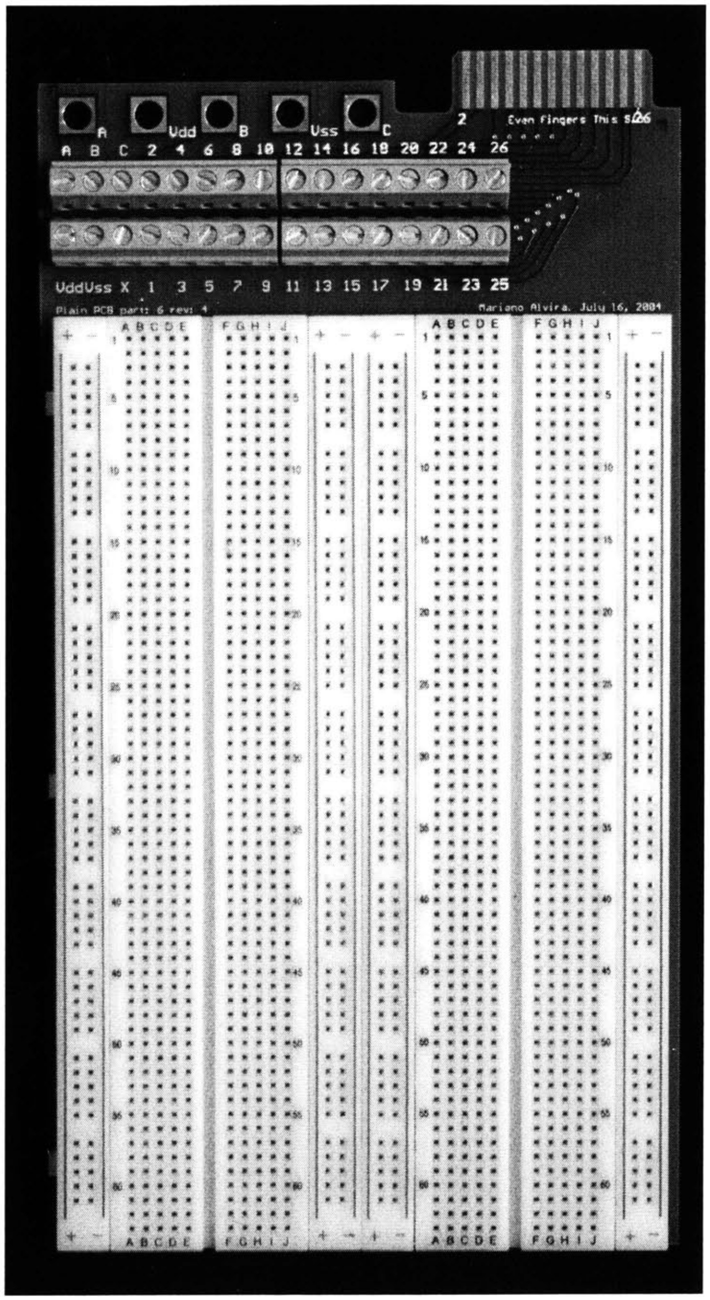

Figure 3.7: The Breadboard Card.

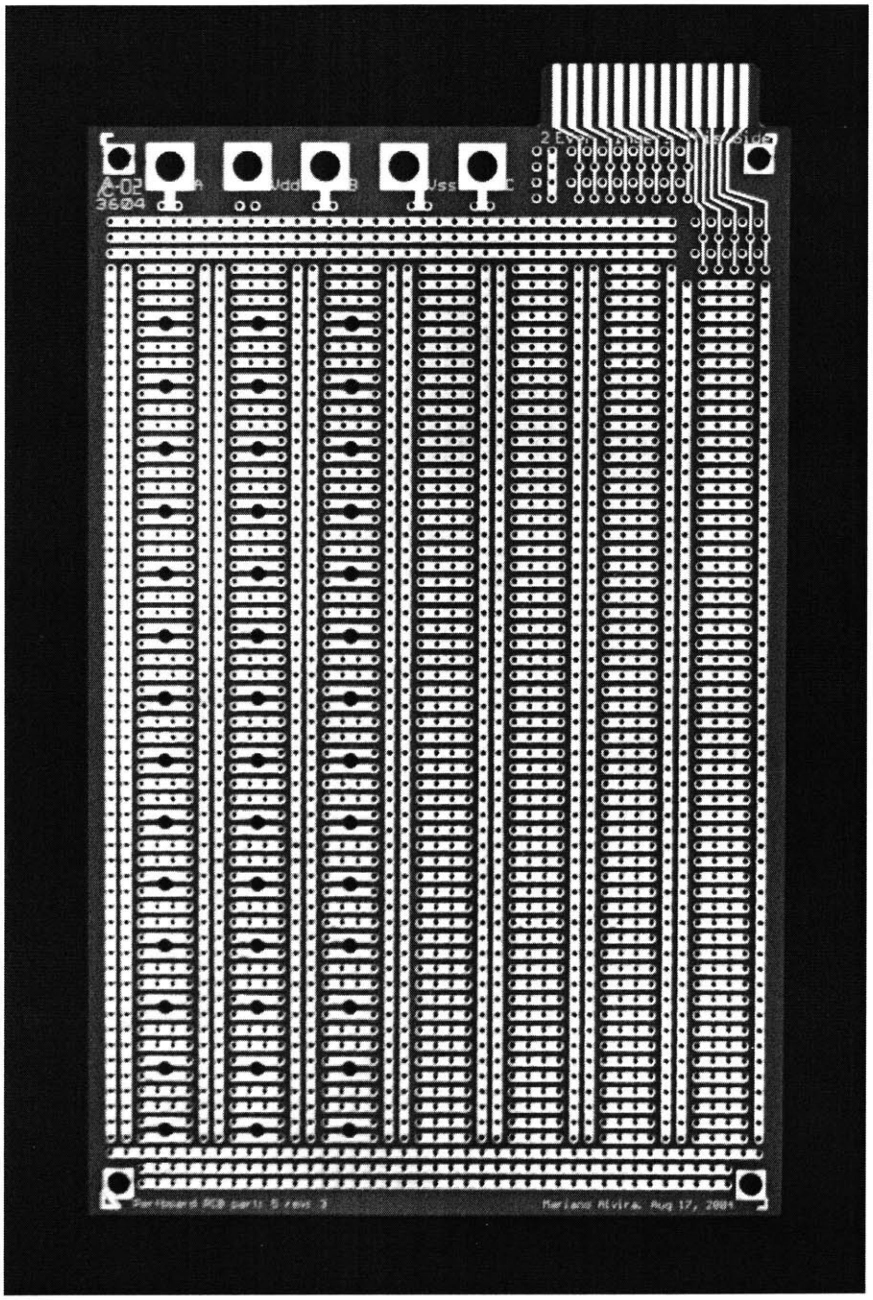

Figure 3.8: The Perfboard Solder Card.

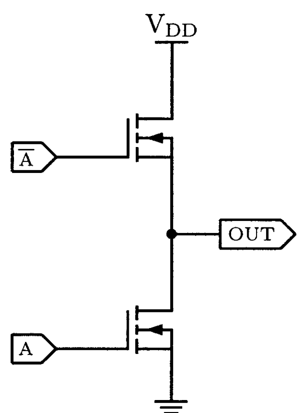

Figure 3.9: The canonical "Totem Pole" with high- and low-side NFETs; a floating gate drive is used for the high-side FET.

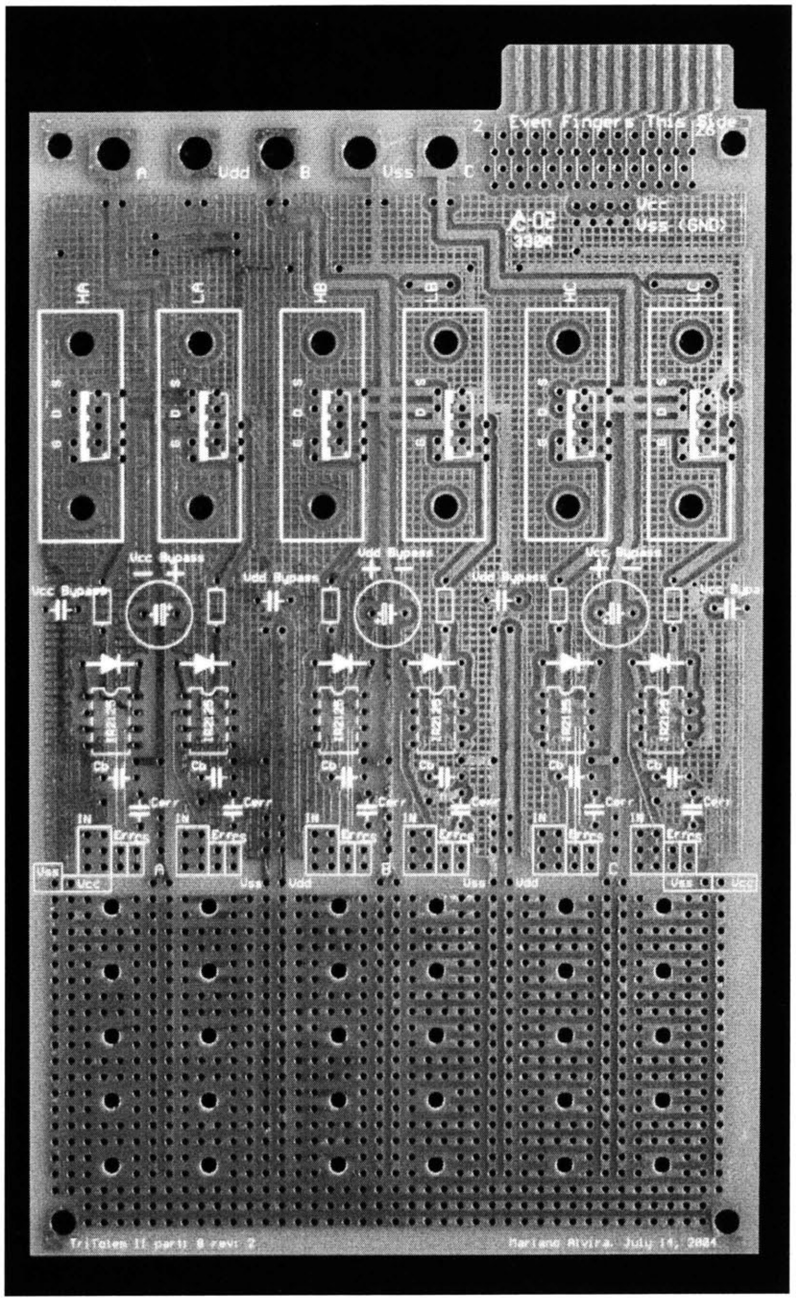

Figure 3.10: The TriTotem II Card.

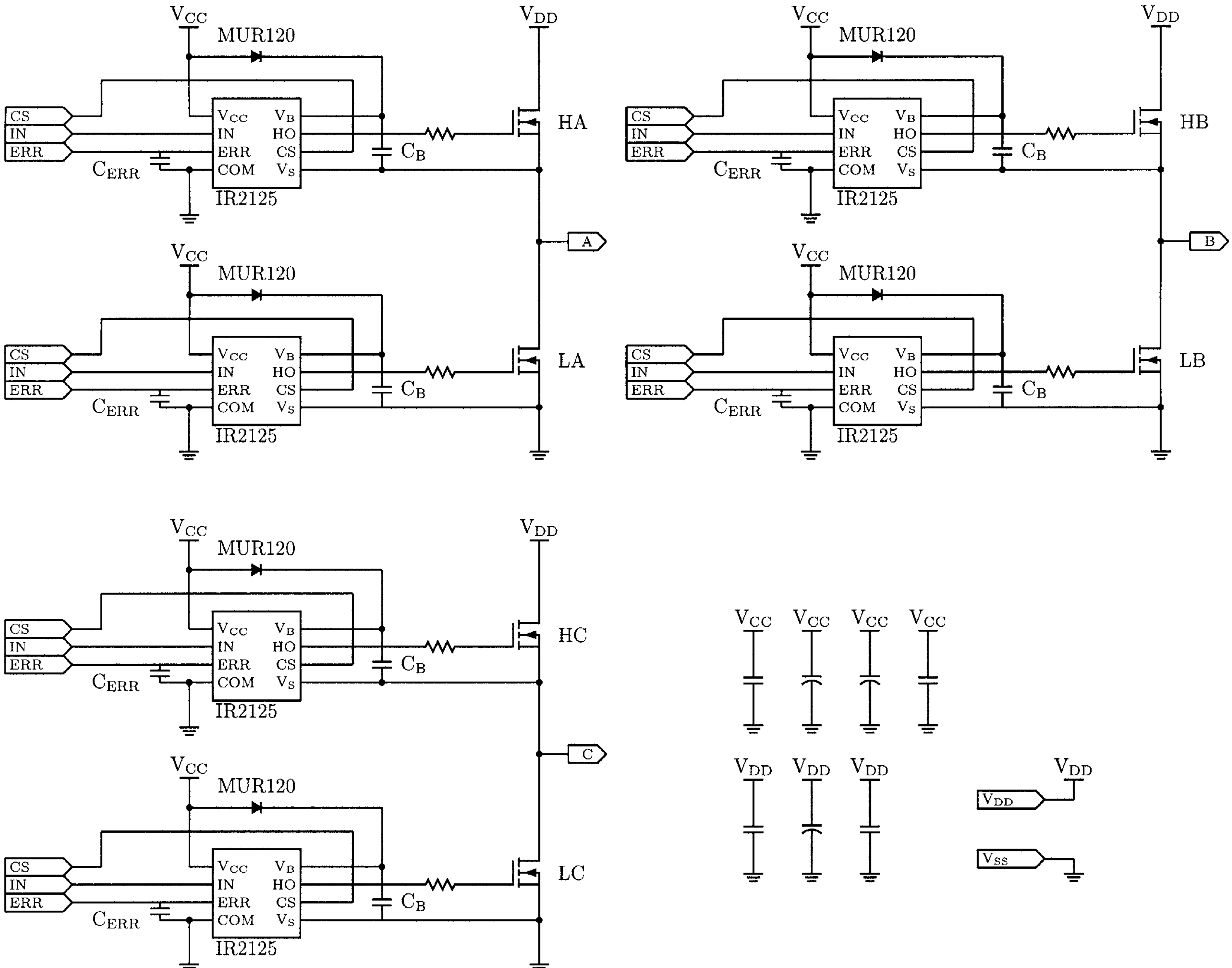

Figure 3.11: TTII schematic.

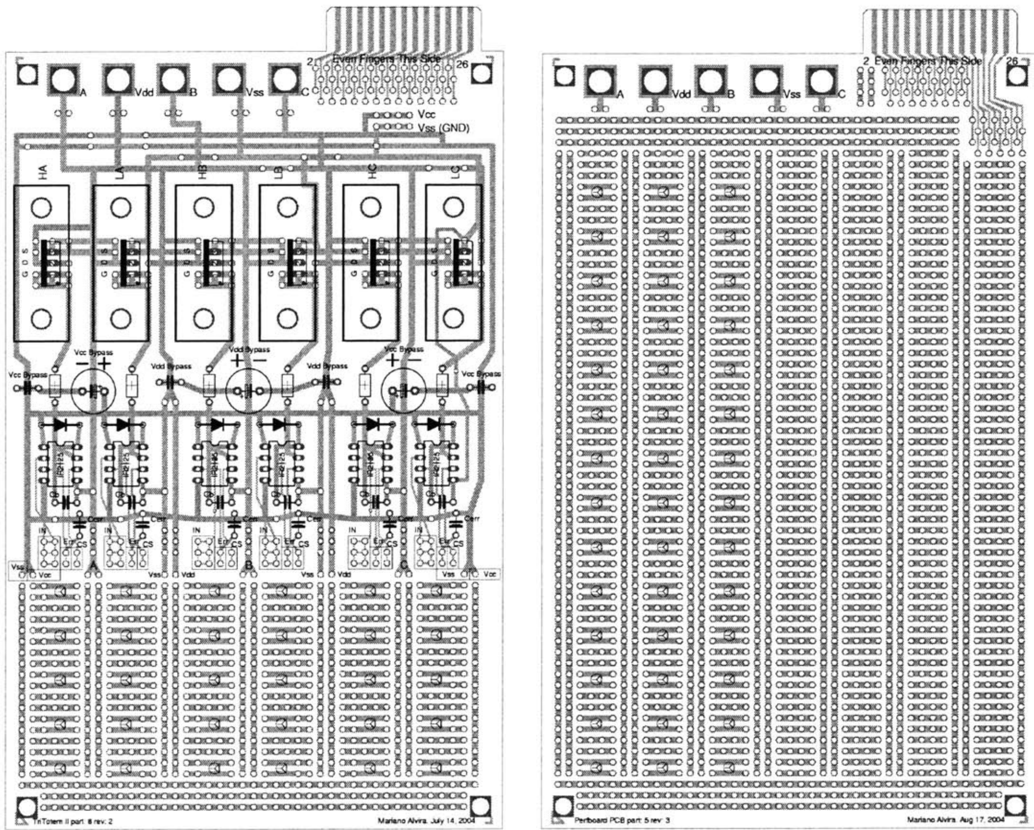

Figure 3.12: The laminated design sheet for the TriTotem II Card and the Solder Card.

Chapter 4

Lab 1: Linear versus Switching Power Converters

THIS chapter presents the first laboratory taught in 6.131 [3]. This lab motivates the need for switching power electronics, and teaches fundamental building blocks the students will use in the exercises that follow [8]. The only prerequisite to 6.131 is a course in circuit fundamentals. Therefore, this first lab starts with analysis of a few voltage converters using resistors and diodes. By building and testing these voltage references, the student discovers that, as more current is drawn from the output the reference voltage drops and the circuit is no longer a good reference. It is shown that these methods of generating one voltage from another work only at low current, and therefore, low power. To convert energy from one form to another at power levels high enough to do useful work requires other circuitry taught in 6.131.

Next, students are challenged to build a linear regulator. This circuit, as before, creates one voltage from another. The student analyzes what happens as various amounts of currents are drawn from the regulator. They find that the linear regulator is much *stiffer* than the references they built previously. But they also discover a new problem — their circuit gets hot; as they draw power from the regulator more power is wasted. By building a linear regulator, they learn that in addition to the problem of *conversion* — how to change one form of energy to another — there is also the question of *efficiency.* In 6.131, students learn to design circuits that can efficiently convert power from one form to another.

Next, they are introduced to several oscillator circuits that can produce square and triangle waveforms that can be used to create pulse width modulated (PWM) switching signals. They are shown a method to create "break before make" switch patterns, where two series switches are both always off, before one turns on (to avoid short circuits). They are also introduced to the IR2125 high-side MOSFET driver, which is a IC used extensively in the rest of the labs to switch MOSFETs.

Once comfortable with the control circuits and MOSFET drivers, the student begins to experiment with switching power converters. Through experimentation, they learn about load averaging, i.e. loads provide a degree of low-pass filtering that causes the output voltage to respond to the average drive, not necessarily the instantaneous waveform. For instance, turning a light on for 50% of a switch cycle is roughly equivalent to applying 50% of full voltage for the whole cycle, so long as the switch cycle repeats often enough. They notice that the switching circuits run cool to the touch, indicating that power is efficiently applied to the load. Finally, the student constructs a switching audio amplifier on breadboard in preparation for when they build a high power version in Lab 2 on a TTII card.

4.1 Voltage References

In this exercise, the student builds and investigates three reference voltage circuits. Each of these circuits takes an input voltage, V_{in}, and produces a lower output voltage, V_{out}. The three circuits — a voltage divider, zener reference, and a diode stack reference (shown in Figures 4.1, 4.2, and 4.3 respectively) — are potential voltage regulators.

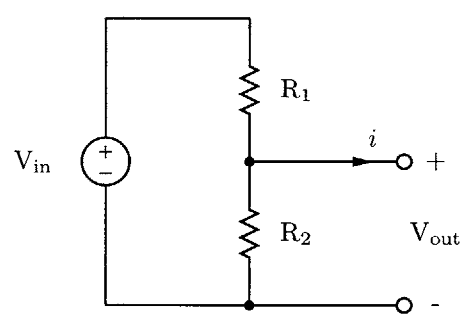

Figure 4.1: Voltage divider reference.

Assuming that V_{in} = 12V and V_{out} = 6V, the student develops a Thevenin equivalent circuit for each reference circuit, and discusses what happens to the output voltage as different load resistors are connected to the output port. For the Zener reference, the student chooses a suitable

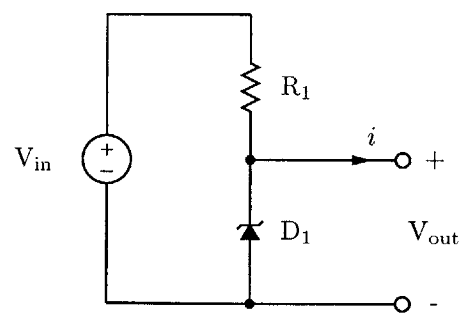

Figure 4.2: Zener diode reference.

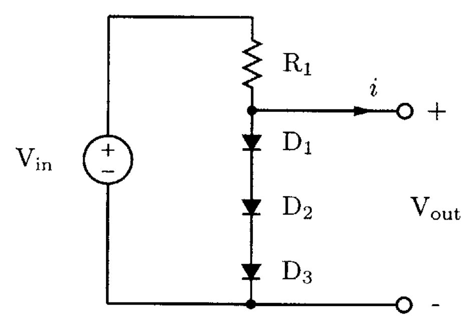

Figure 4.3: Diode stack reference.

diode from a table of Zener diode specifications, and for the diode stack reference, they are told to use an appropriate number of 1N4148 diodes. They are also asked to discuss the efficiency of each circuit, that is, as power is delivered to the load, what happens to the overall power consumed by the circuit. The student learns that the output voltage generated in each of these circuits drops substantially as current is drawn by the load. They also learn that they are not particularly efficient, as each of these circuits has a resistive element that drops the input voltage to the desired output level.

These circuits begin to teach key lessons in 6.131, and they also familiarize the student with 6.131's emphasis on design and analysis, rather than copying circuits from building instructions. That is not to say, however, the students must design everything from scratch. They are given the tools to get going, but key design decisions are left up to them. For more complicated projects, such as a switching power converter, the students' designs are reviewed by the staff, and any errors in the design are corrected during this review so that the student can proceed to build their circuit successfully.

4.2 Linear Power Amplifiers

In this exercise the student constructs two types of linear regulators. In the previous exercise, they found that the voltage reference circuits worked well for low output current. They start this next exercise by isolating a divider reference from a load resistor with an op-amp buffer, as shown in Figure 4.4. This circuit teaches the student a common way to isolate one circuit from another. They see that in this circuit, V_{out} holds at the desired level, for any R_L, so long as the output current rating of the op-amp is not exceeded. Using a LM358 as the op-amp, the student determines what the minimum value R_L can have such that V_{out} remains at the desired output voltage. Since the LM358 has a maximum output current of 20mA, the lowest R_L is 300 Ω (for V_{out} = 6V).

The student then builds the circuit shown in Figure 4.5, using a 40N10 MOSFET, and implements the voltage divider with a 20 kΩ potentiometer. They then connect a 20 Ω load resistor and learn that with the addition of the output FET, this circuit can provide several amps to the load and still maintain the desired output voltage.

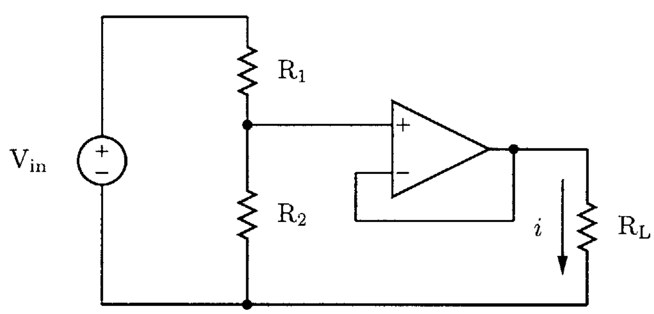

Figure 4.4: Voltage divider reference isolated with an op-amp buffer.

The student tests the linear power supply shown in Figure 4.5 on loads provided by the LoadBoy test suite, shown in Figure 4.6. LoadBoy provides: two 12V taillights, two 6W speakers, and two DC motors coupled together so that one drives the other (a motor/generator pair). The DC motors also have tachometers that output a voltage proportional to the angular velocity of the shaft. While testing their circuit, the student learns how the different loads operate. For instance, they learn that the brightness of the light bulbs depends on the voltage applied to them, and similarly, that the angular velocity of the motors varies in proportion to the output voltage.

They also measure the efficiency of the linear regulator for various output voltages. By

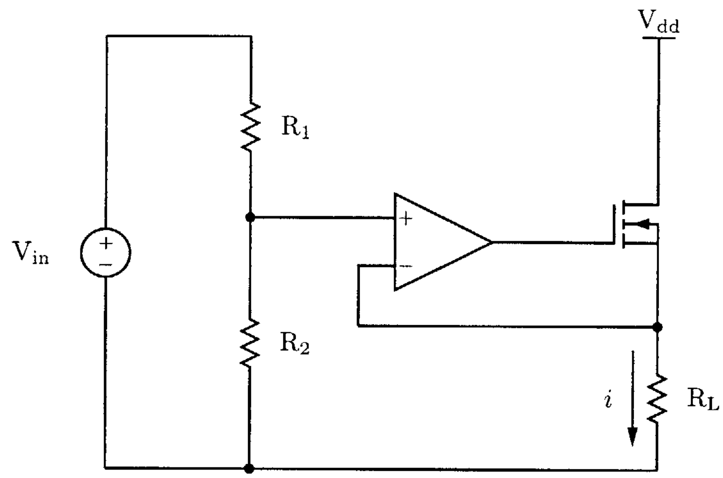

Figure 4.5: Op-amp buffer with MOSFET to boost output current.

plotting efficiency versus output voltage they learn that for the linear regulator, efficiency is directly proportional to output voltage. The poor efficiency of a linear regulator if further shown by the heat the MOSFET generates.

4.3 Oscillators, Pulse Width Modulators, and Delay Circuits

The efficiency of the linear regulator is poor because the MOSFET operates in a regime where it has both a voltage across it and a current through it. Operated as a switch, however, one of these quantities is close to zero, and the MOSFET wastes significantly less power. In this next exercise the student builds three circuits that will be used to control MOSFETs as switches: oscillators, pulse width modulators (PWM), and delay circuits. The oscillators produce a periodic waveform that indicates the start and stop of a switching cycle. A PWM circuit uses an oscillator to adjust the portion of the cycle where the switch is turned on. The delay circuits allow two switches to be controlled in a "break before make" pattern, to avoid short circuits.

The three oscillators shown in Figures 4.7, 4.8, 4.9, work in similar ways. The capacitor voltage charges up to a high voltage threshold, which causes the output to change and then the capacitor discharges to a low voltage threshold. When that threshold is reached, the output changes and the cycle repeats. If the circuit in Figure 4.7 is implemented with a 74HC14, then the high threshold, v_{th}, and the low threshold, v_{tl}, are equal to 2/3 and 1/3 of the supply voltage, respectively,

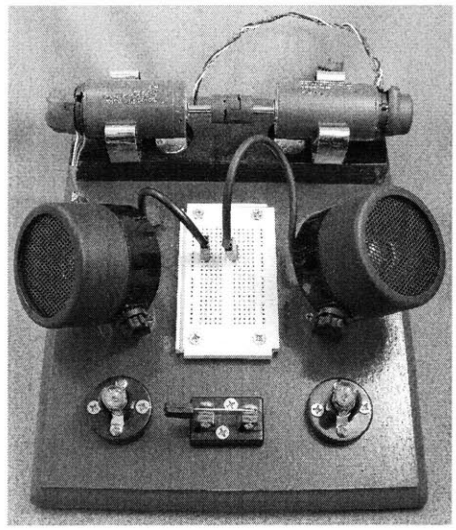

Figure 4.6: The LoadBoy test suite.

just as in a 555 timer. The circuit in Figure 4.8 has a different charging and discharging pathway, allowing for different duty cycles. Adding the diode in Figure 4.9 is another way to produce different duty cycles. The Schmitt trigger oscillator can also produce different duty cycles for the output with additional resistors and diodes.

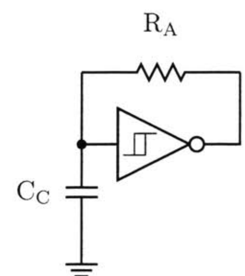

Figure 4.7: A relaxation oscillator using one gate of a 74HC14.

An advantage of these oscillators is that for properly sized resistors and capacitors, the capacitor voltage approximates a triangle wave. By comparing this triangle wave to an adjustable DC level, it is possible to create and PWM waveform with an adjustable pulse width as shown in Figure 4.10.

A PWM waveform and its inverse can be used to control the two switches in a totem pole. Typically, one MOSFET is driven with the PWM signal, and the second MOSFET is driven with

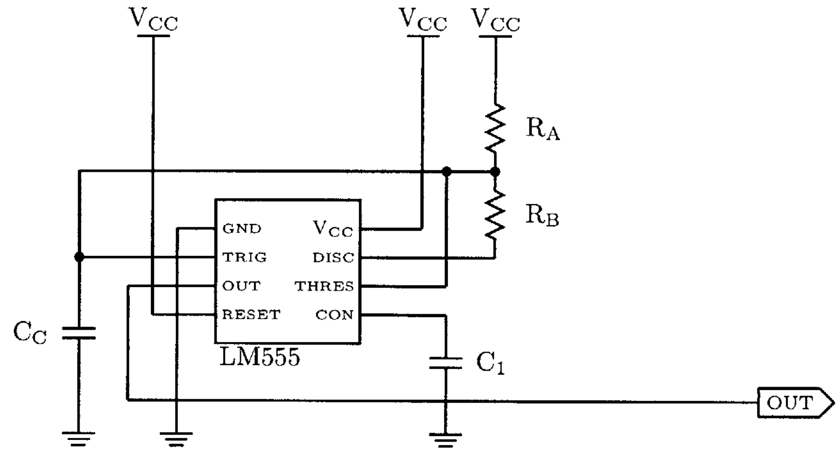

Figure 4.8: 555 timer connected for astable operation.

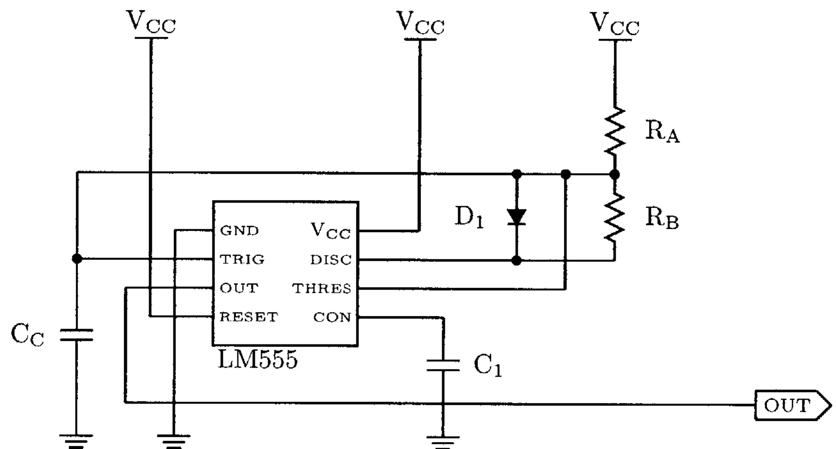

Figure 4.9: 555 timer connected for astable operation using a diode to effect the duty ratio.

an inverted version of the signal. The intention is that both MOSFETs are never on at the same time. It takes time, however, for the MOSFETs to switch state. Therefore, it is necessary to create "dead-time", where both switches are off, at the edges of the PWM signal. The operation of one such delay circuit is illustrated in Figure 4.11.

This circuit takes an input switching command and creates two output signals, one for each switch. The rising and falling time delays, t_{dr} and t_{df} respectively, are set by the resistor and capacitor in each circuit. The circuit on the left charges the capacitor through the resistor on a rising edge of v_2, while the circuit on the right is sensitive to a falling edge. A similar result can be obtained with diodes facing the same direction, however, this method uses seven gates. The configuration shown only uses five gates (out of six on a single 74HC14), this leaves one gate free

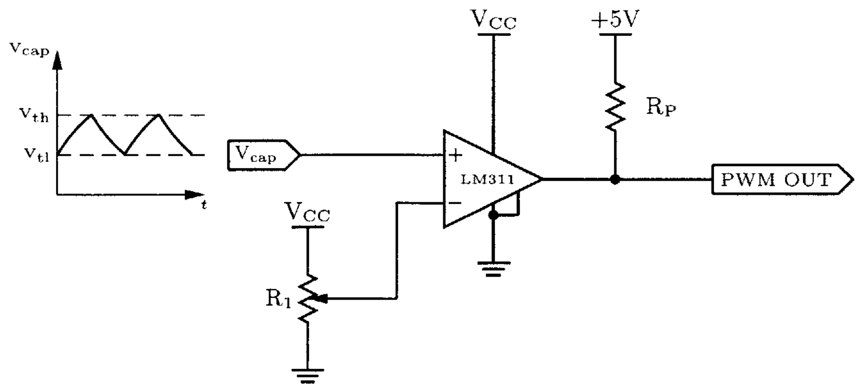

Figure 4.10: Using an LM311 to create an adjustable duty ratio.

to be used as an oscillator like the one in Figure 4.7. Using only two ICs, a 74HC14, and a LM311, one can create a full control circuit for a totem pole with an adjustable duty cycle.

4.4 Switching Power Amplifier

In this exercise, the student constructs the switching supply shown in Figure 4.12. By powering various loads on LoadBoy with different duty ratios, the student discovers that the loads filter the switching waveform and respond to the average voltage of the signal. Thus, the tail-light driven with a 50% duty ratio appears to be at reduced brightness even though full voltage is applied to the light for part of the cycle.

Next the student adds a high-side MOSFET and creates the complete totem pole shown in Figure 4.13, and tests it with a load resistor. Once the drivers and delays circuits work, the student adds an oscillator and LM311 to create a PWM signal. The PWM generator is set to produce a nominal duty ratio of 50%. The student capacitively couples an audio signal on to the duty ratio command voltage, modulating the output duty ratio according to the audio signal. When the load resistor is replaced with a speaker on LoadBoy, and the student can enjoy music on this switching audio amplifier. The completed circuit is show in Figure 4.14.

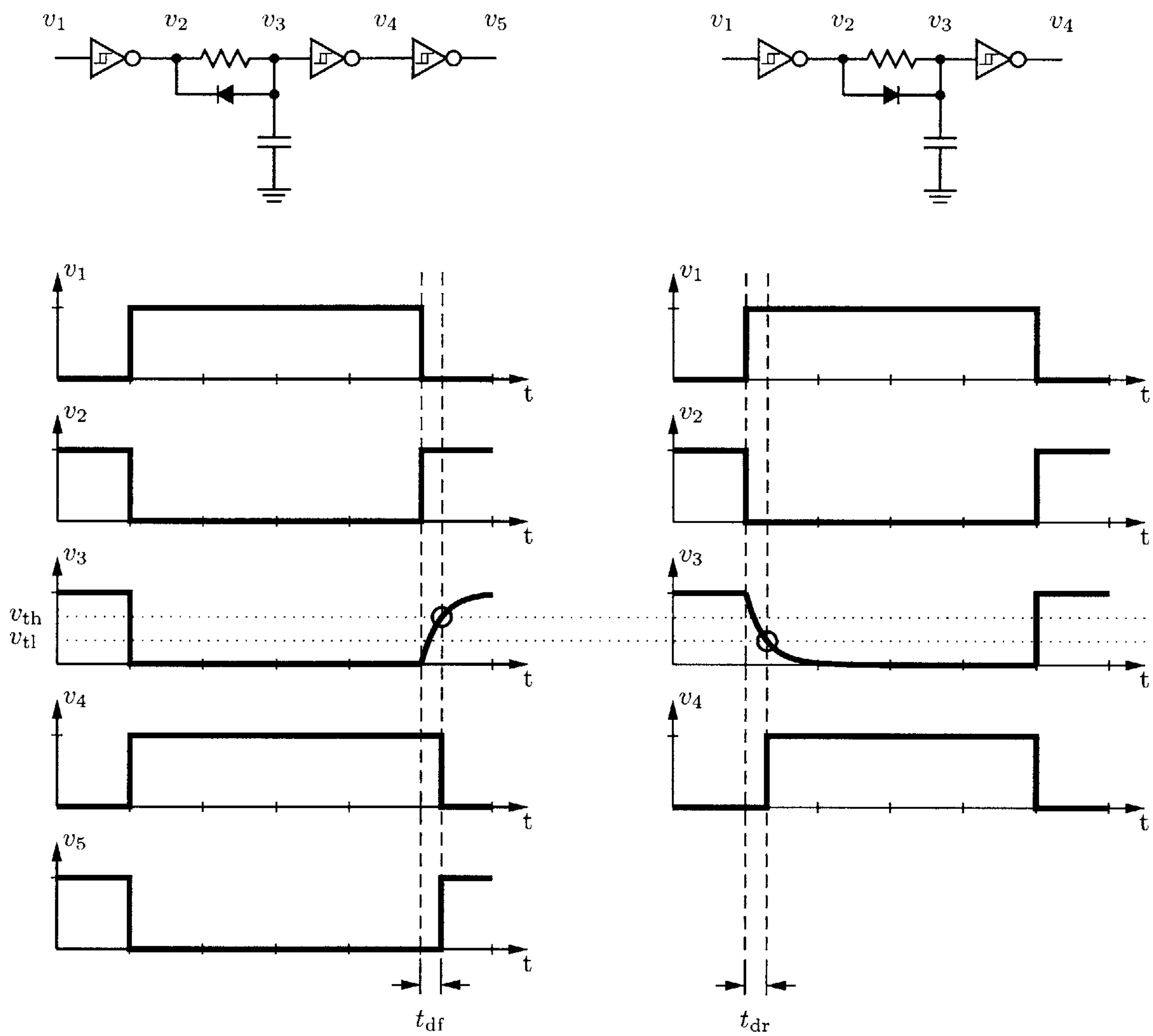

Figure 4.11: Using five gates of a 74HC14 to create a "break before make" switching waveforms.

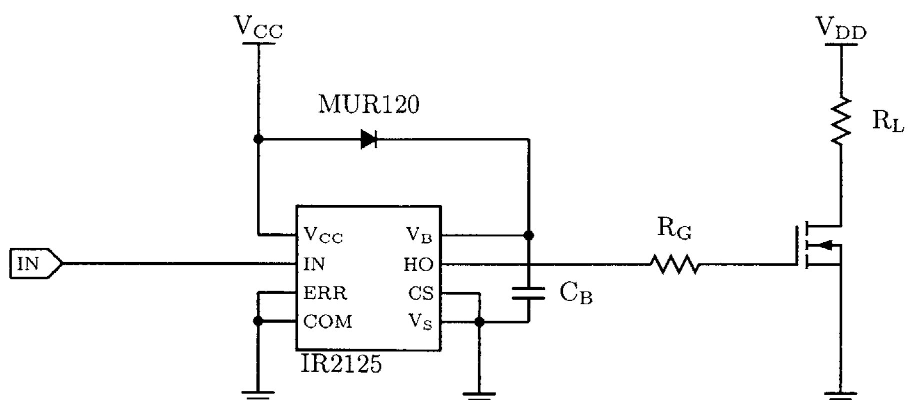

Figure 4.12: Using an IR2125 for drive a low-side MOSFET.

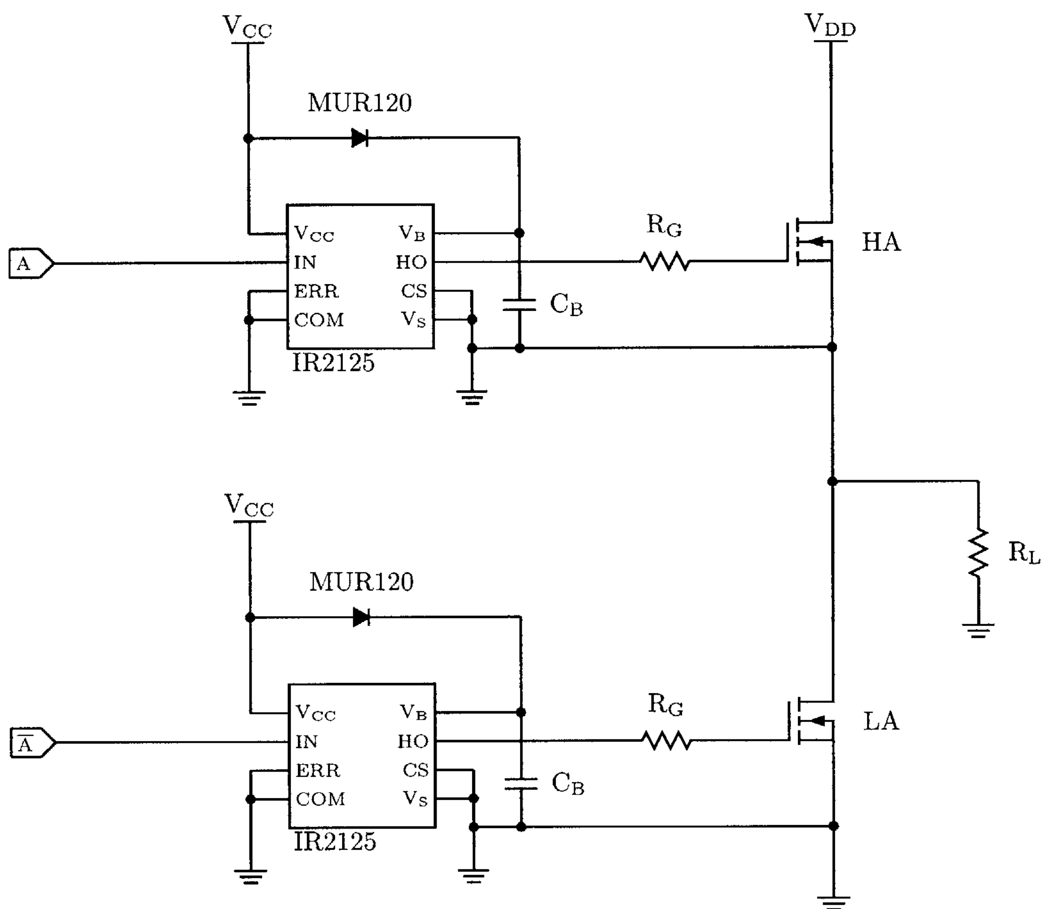

Figure 4.13: Using two IR2125s to drive a high- and low-side MOSFET pair.

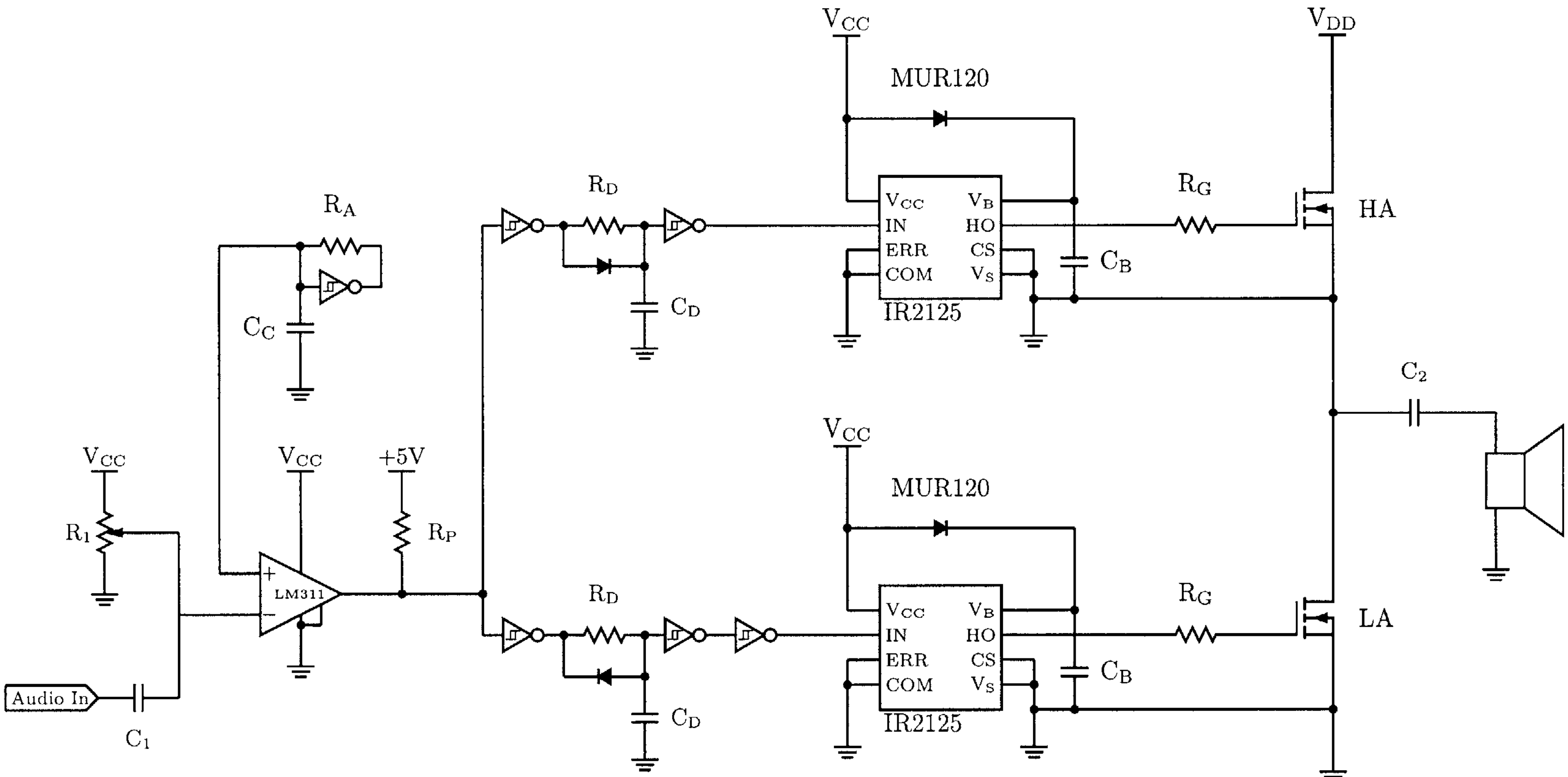

Figure 4.14: Full schematic for the 6.131 audio amplifier.

Chapter 5

Lab 2: Switching Converters

THE exercises in the second lab concentrate on design switching power converters [4]. Specifically, the student is walked through a design and construction of a buck converter drive for the 6.131 electric go-kart. While they are working on this, they also design a 12W, portable power supply for a switching stereo amplifier. Upon completion of a "design review", discussed in Chapter 8, they are cleared to build their power supply on a second TTII PCB, as well as a two channel version of their audio amplifier from Lab 1 on a third TTII PCB.

The go-kart is the highest power system presented in the class. The go-kart drive must supply 500W continuously, and up to a 1500W surge during acceleration. At these power levels, poor designs fail dramatically. The student must show their working go-kart supply on the bench, to a staff member, before the staff helps them run the go-kart. This level of staff involvement is necessary to ensure safety and a good learning experience. The go-kart exercise is a key opportunity for the staff to work one-on-one with students, developing their design and assembly skills.

For the stereo supply, the student is given more freedom to design. The lab exercise provides a topology and a few specifications to work from; however, the choice of components and control circuits is up to them. The specifications have been cleverly designed to lead the student to some illuminating trade-offs that can be discussed during the design review. The design process is not handed out, but must be discovered, together with the teaching staff.

5.1 Go-kart Power Supply

This section describes the design of a buck converter that can drive the 6.131 go-karts at variable speeds. The design process shown here is presented in lecture as a "warm-up" exercise so that students can understand how to arrive at the design and so that they can apply a similar method when designing the power supplies for their stereo.

The 6.131 go-kart is shown in Figure 5.1. The battery compartment under the seat contains three lead-acid batteries providing 36V to operate the go-kart. The go-kart includes a 1.5 HP DC motor connected to the rear wheel with a chain drive link. The motor has a tachometer and cooling fan. The steering wheel has two switches, a push-button, and a throw switch, as well as a slide potentiometer. The electrical terminals for all of the go-kart components convene in the tool-box mounted on the back of the go-kart; this is where a Power NerdKit can be inserted. The battery and motor connections penetrate the tool-box through four banana plugs, which are connected inside to wires with ring lugs. The low-power components, like the switches and slide pots, enter the tool-box through DB-25 connector. Inside the box, these connections are accessible via DIP connector with the pin-out shown in Figure 5.2.

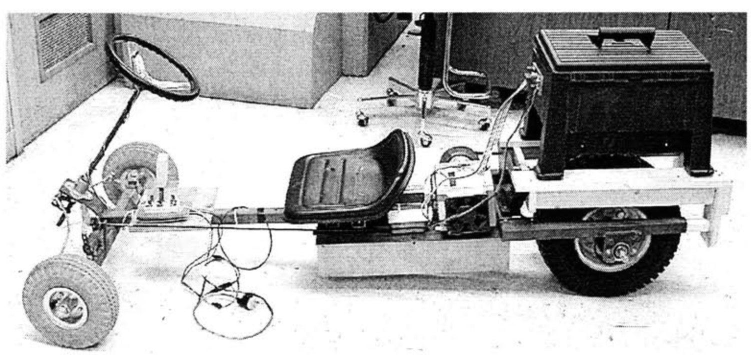

Figure 5.1: 6.131 Go-kart.

The power consumption and motor currents for a variety of operating modes are shown in Table 5.1. The cruising condition occurs once the go-kart has fully accelerated and maintains its top speed for that drive voltage; this is the case where the minimum current is drawn from the supply for a given drive voltage. Similarly, the stalled case occurs when the go-kart is driven, but not moving; this is the case where the maximum current is drawn from the supply.

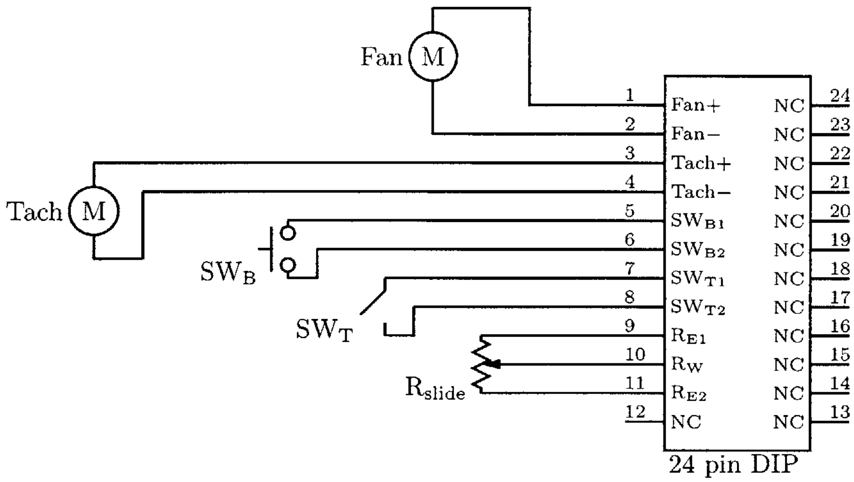

Figure 5.2: Pinout of the DIP connector containing the low power go-kart connections.

Drive Voltage	Quarter (9V)	Half (18V)	Full (36V)
Cruise	13.5W @ 1.5A	54W @ 3A	216W @ 6A
Stalled	81W @ 9A	324W @ 18A	1300W @ 36A

Table 5.1: Operating modes of the Go-Kart buck.

This table shows that the worse-case current, from a stalled go-kart with full drive voltage, is 36A. Our circuitry must be able to handle this current continuously, for safety reasons. As mentioned before, the TTII can handle this current if reinforced traces are used.

The FETs typically used in 6.131 are 40N10s which, when running hot (150 °C), have an ON resistance of 80 mΩ. The course staff stocks a heatsink with a thermal resistance of 10°C/W. The junction thermal resistance adds an additional 5°C/W, giving a total thermal resistance of 15°C/W. With a generous 100°C rise above ambient temperature, the FET can dissipate up to 6.67W on average. In the high-side FET, the power dissipated is

$$\langle P_H \rangle = D \cdot I_L^2 \cdot R_{DS,ON} \tag{5.1.1}$$

and in the low-side FET, the conduction power loss is

$$\langle P_L \rangle = (1 - D) \cdot I_L^2 \cdot R_{DS,ON} \tag{5.1.2}$$

Considering the worse case, a stalled motor appears as a load of 1 Ω. Therefore

$$I_L = DV_I \tag{5.1.3}$$

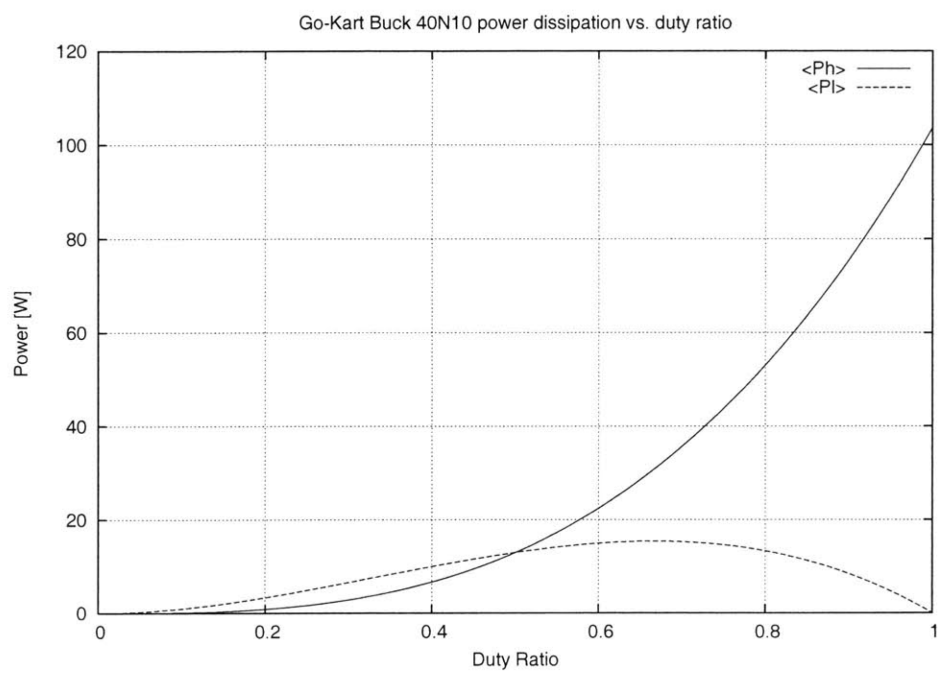

Figure 5.3: Power dissipation in each FET of the Go-Kart buck as a function of duty ratio.

Figure 5.3 graphs the power dissipated in the high- and low-side FETs as a function of the duty ratio D. This graph shows that the low-side FET is the first to reach 6.5W at D=0.3, corresponding to an current of 11A. This is too low to quickly bring the go-kart up to cruising speed, and thus a MOSFET with a lower $R_{DS,ON}$ is needed. The IRF1407 has an $R_{DS,ON}$ of 16 mΩ when hot. Using this MOSFET, then the high side will dissipate 6.5W at D=0.86. This corresponds to a more aggressive 31V drive voltage which will quickly accelerate the go-kart to cruising speed.

A complete schematic of the power supply is shown if Figure 5.4. The student is free to choose any method they wish to generate the 30kHz switching frequency, and any method to create 500ns to 1μs of shoot-through delay. The speed of the go-kart is controlled with the potentiometer on the steering wheel, R_{slide}. The student sets the values of R_A and R_B such that the maximum duty ratio is 0.8. This prevents the MOSFETs from overheating, as well as, ensuring that the high-side bootstrap capacitor, C_B, is refreshed every switching cycle.

5.2 Buck Converter Analysis

This section presents an analysis of a buck converter and develops the design equations necessary to build the go-kart and stereo buck converters. More in depth analysis of this converter can be found in [2] and [7].

The high-side MOSFET in the buck converter of Figure 5.5 is switched ON with duty ratio D. When the high-side FET is ON the low-side is OFF, and vice versa. Assuming that the converter is in periodic steady state (PSS), then the average inductor voltage, $\langle v_L \rangle$, is zero. Therefore

$$\langle v_X \rangle = V_o$$

The average voltage across the low-side FET is also

$$\langle v_X \rangle = DV_i$$

thus, solving for D yields

$$\frac{V_o}{V_i} = D \tag{5.2.1}$$

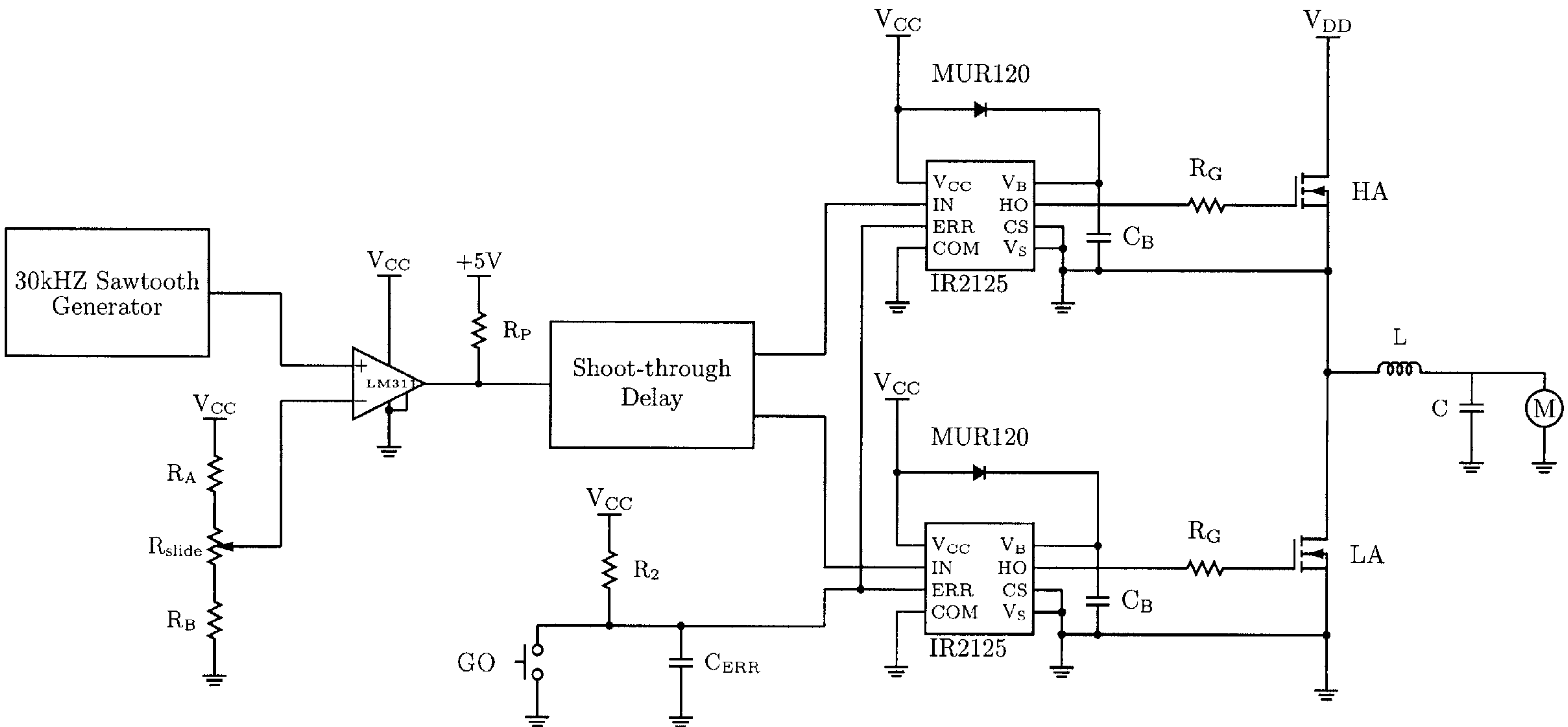

Figure 5.4: Scematic of the go-kart power supply.

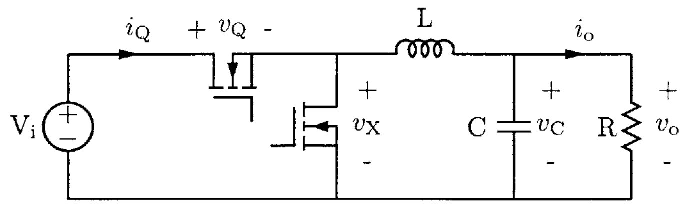

Figure 5.5: The basic buck converter.

The magnitude of the inductor ripple current is

$$|i_L| = \frac{(V_i - V_o)DT}{L} = \frac{V_o(1-D)T}{L} \tag{5.2.2}$$

In order to remain in CCM, i_L must not reach zero. Or, in other words, the average inductor current must always be greater than half of the inductor ripple current:

$$\langle i_L \rangle > \frac{|i_L|}{2} \tag{5.2.3}$$

substituting for the magnitude of the inductor ripple current gives

$$\langle i_L \rangle > \frac{V_o(1-D)T}{2L} \tag{5.2.4}$$

and then substituting $D = \frac{V_o}{V_i}$

$$\langle i_L \rangle > \frac{V_o(1-\frac{V_o}{V_i})T}{2L} \tag{5.2.5}$$

5.3 Go-kart Output Filter

A large iron-powder core is used for the output filter of this converter, due to the large DC currents involved. Iron-powder is an ideal material for this application as it softly saturates, that is, its permeability declines gradually with increasing flux density. Therefore, a core that provides good filtering at cruising currents can be used, and during intense accelerations it will still provide adequate filtering — despite the heavy amounts of current. The inductor constructed uses 90 turns of 18 gauge wire on T-400-52 core from Micrometals. This inductor provides about 800μH at 5.5A, and 160μH at 36A. A 20μF paper film capacitor was used, which has good frequency response up to 30kHz. This filter has a nominal breakpoint at 1.1 kHz. At 36A the breakpoint is at 3.6kHz, which still provides adequate filtering of 30kHz.

5.4 Portable Stereo Power Supply

After working through the variable speed go-kart drive, the student then designs and builds a power supply suitable for a 12W stereo. This supply takes an input voltage of 4-6V and raises it to 15V with a boost converter. That voltage then powers a buck converter with an adjustable output voltage. The buck converter powers the rails of the stereo, thereby controlling the output voltage of the buck converter controls the volume of the music. The suggested topology for this supply is shown in Figure 5.6. Using this topology allows the supply to be built on one TTII card.

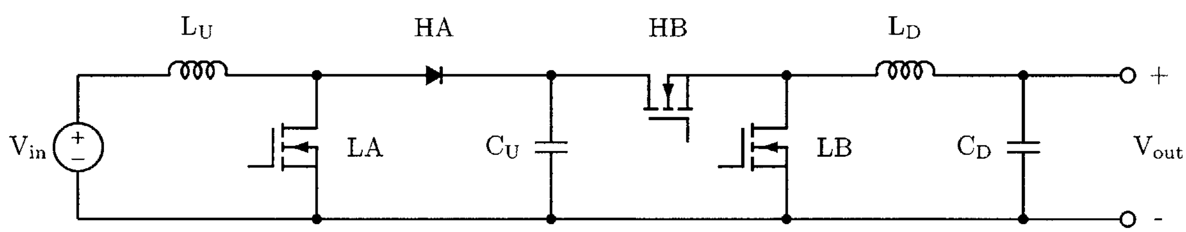

Figure 5.6: Suggested topology for the stereo power supply.

5.5 Stereo Supply Buck Converter

The stereo consists of two switching audio amplifiers from Lab 1 on a TTII PCB. Then the amplifier is powered by a buck converter that meets the following specifications:

Specification	Value	Unit
Input Voltage:	12	V
Switching Frequency:	250	kHz
Output Power:	12	W
Min. Efficiency:	0.7	
Min. load for CCM: $V_{out} = 12V$ $R_L = 12\ \Omega$	0.12	W
Output Filter Max Breakpoint:	200	kHz
Output Ripple:	1.2	V
$\lvert i_{out}\rvert = 1A$		
i_{out} min freq:	500	Hz
i_{out} max freq:	10	kHz

The output ripple regulation required for the given frequency band is necessary for adequate sound quality. Starting with the CCM requirement, (5.2.5) can be rewritten to yield an expression of the minimum L for a given $\langle i_L \rangle$. Thus,

$$L > \frac{V_o(1 - \frac{V_o}{V_i})T}{2\,\langle i_L \rangle}$$

substituting with the values specified

$$L > \frac{12V \cdot (1 - \frac{12V}{15V}) \cdot 4\mu s}{2\frac{12V}{12\Omega}}$$

or

$$L > 4.8\mu H \tag{5.5.1}$$

Considering the output voltage ripple specification, the output impedance of the buck converter is modeled as a parallel inductor and capacitor with effective series resistance. Thus:

$$Z_o = \frac{s^2LCR_C + s(L + R_LR_CC) + R_L}{s^2LC + s(R_CC + R_LC) + 1} \tag{5.5.2}$$

For $R_C = R_L = 0.01\ \Omega$, setting $\frac{1}{\sqrt{LC}} = 250$Hz results in $Z_o = 1$ at approximately 300Hz. Therefore, 1A of output ripple current results in 1V of output ripple voltage, which is better performance than specified. Using the largest capacitor stocked, 2000 μF, sets L = 200 μH.

The core for L and be selected using the graph shown Figure 5.7. Using specifications for various Micrometals cores, this graph parameterizes the inductance and saturation current in terms of an integer number of turns. The saturation current is defined to be the current such that the effective permeability of the material is at 80% of its nominal value. The Octave code to produce this and other charts for other cores is included in Appendix C.

At maximum loading, L carries 1A. From Figure 5.7 that a T72-26 or larger can create a 200 μH inductor that can carry at least 1A. The reference design uses a T90-26 core with 54 turns of 24 AWG wire.

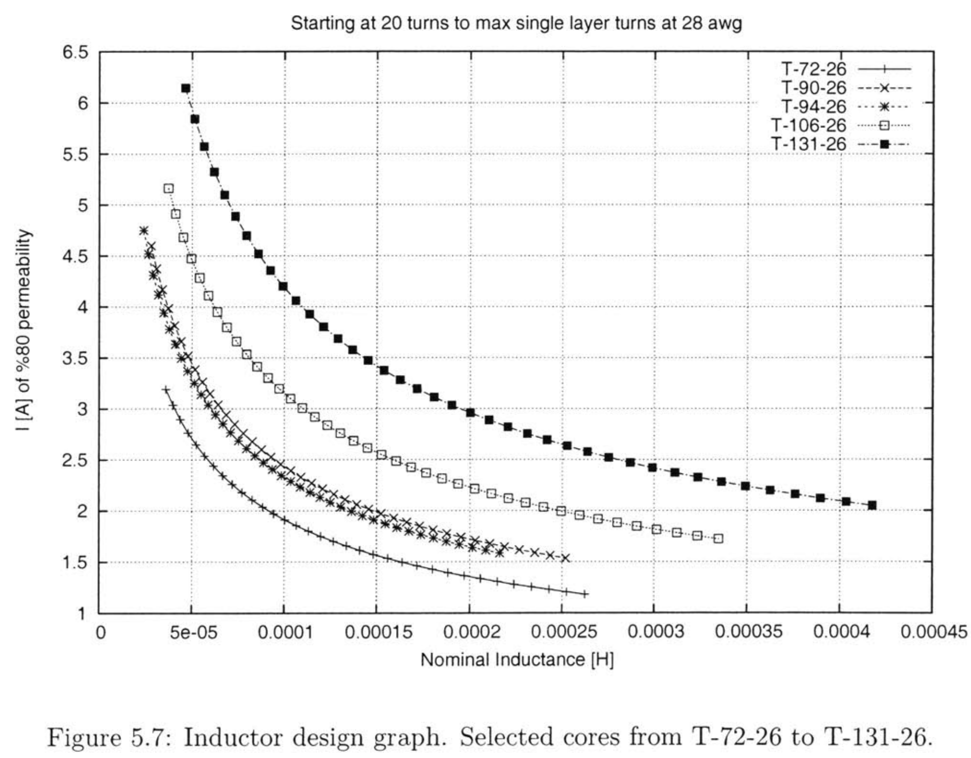

Figure 5.7: Inductor design graph. Selected cores from T-72-26 to T-131-26.

5.6 Stereo Supply Boost Converter

The lab exercise specifies the following set of requirements for the boost converter:

Specification	**Value**	**Unit**
Input Voltage:	4-6	V
Output Voltage: $V_{in} = 6V$	15	V
Switching Frequency:	250	kHz
Output Power:	17	W
Min. Efficiency:	0.7	
Min. load for CCM:	0.25	W
Output Ripple: full output power	1.2	V
Max. Capacitor Impedance: @ 10 kHz	0.1	Ω

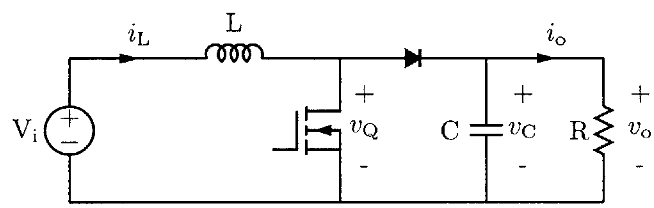

Figure 5.8: The basic boost converter.

A basic boost topology is shown in figure 5.8. The MOSFET is switched with a duty ratio D. Assuming PSS, then

$$\langle v_Q \rangle = V_i \tag{5.6.1}$$

as $\langle v_Q \rangle = V_o(1 - D)$, then the conversion ratio is

$$\frac{V_o}{V_i} = \frac{1}{(1 - D)} \tag{5.6.2}$$

and solving for the duty ratio yields

$$D = 1 - \frac{V_i}{V_o} \tag{5.6.3}$$

The magnitude of the inductor ripple current is

$$|i_L| = \frac{V_i DT}{2L} \tag{5.6.4}$$

and as before, for the buck converter, to remain in CCM

$$\langle i_L \rangle > \frac{|i_L|}{2} \tag{5.6.5}$$

thus substituting, the CCM condition on the size of L is

$$L > \frac{V_i DT}{2\langle i_L \rangle} \tag{5.6.6}$$

The output voltage ripple is due to the capacitor discharging through the load while the MOSFET is on. While the switch is on, the output voltage discharges through the load with an RC time-constant. Assuming a long time-constant relative to the switching frequency, then the magnitude of the output voltage ripple is

$$|V_o| = \frac{V_o DT}{RC} \tag{5.6.7}$$

The average inductor current is

$$\langle i_L \rangle = \frac{P_{in}}{V_{in}} = \frac{24W}{6V} = 4A \tag{5.6.8}$$

assuming worse-case efficiency.

Substituting the desired conversion ratio into (5.6.3), yields the duty ratio

$$D = 1 - \frac{6V}{15V}$$

or

$$D = 0.60 \tag{5.6.9}$$

Using (5.6.6), the minimum L to sustain CCM is

$$L > \frac{6V \cdot 0.6 \cdot 4\mu s}{2 \cdot \frac{0.25W}{6V}}$$

or

$$L > 170\mu H \tag{5.6.10}$$

Using a parametric core graph as before, shown in Figure 5.9 cores larger than T90-52 will provide adequate inductance for 4A of average current, for inductances between 200 μH and 400 μH. The reference design uses a 42 turns on a T106-52 core.

Solving for the capacitance C yields

$$\frac{1}{sC} = \frac{1}{2\pi C \cdot 10kHz} = 0.1\Omega \tag{5.6.11}$$

or

$$C = 160\mu F \tag{5.6.12}$$

A typical choice for C, therefore, is 220 μF, as this is the closest capacitor to 160 μF stocked. Finally, (5.6.13), is used to check that this value of C satisfies the output ripple voltage specification,

$$|\mathrm{V_o}| = \frac{15\mathrm{V} \cdot 0.6 \cdot 4\mu\mathrm{s}}{\frac{(15\mathrm{V})^2}{17\mathrm{W}} \cdot 220\mu\mathrm{F}} \tag{5.6.13}$$

or

$$|\mathrm{V_o}| = 12\mathrm{mV} \tag{5.6.14}$$

which is within specifications.

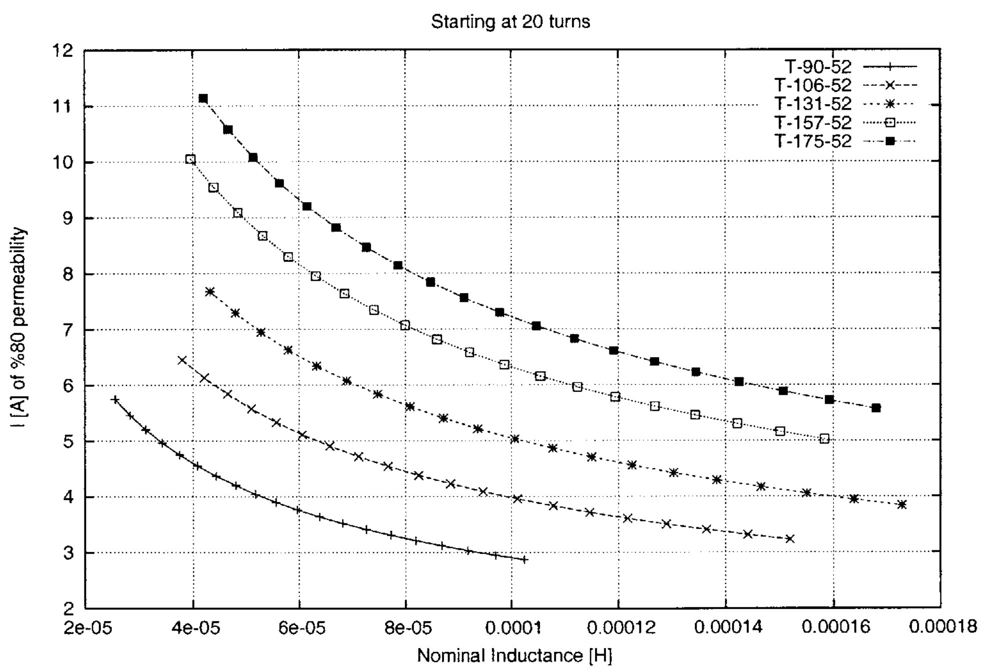

Figure 5.9: Inductor design graph. Selected cores from T-90-52 to T-175-52.

5.7 Boost Start-up Circuit

The topology shown in Figure 5.6 can be successfully tested on the bench. However, in order for the boost MOSFET drivers to function, they must be powered by at least 12V. This circuit presents students with a very real problem in power electronics — start up sequencing. To test the supply, the student can power the IR2125s with a separate lab supply. As the final step in construction the lab exercise suggests the boost priming circuit shown in Figure 5.10.

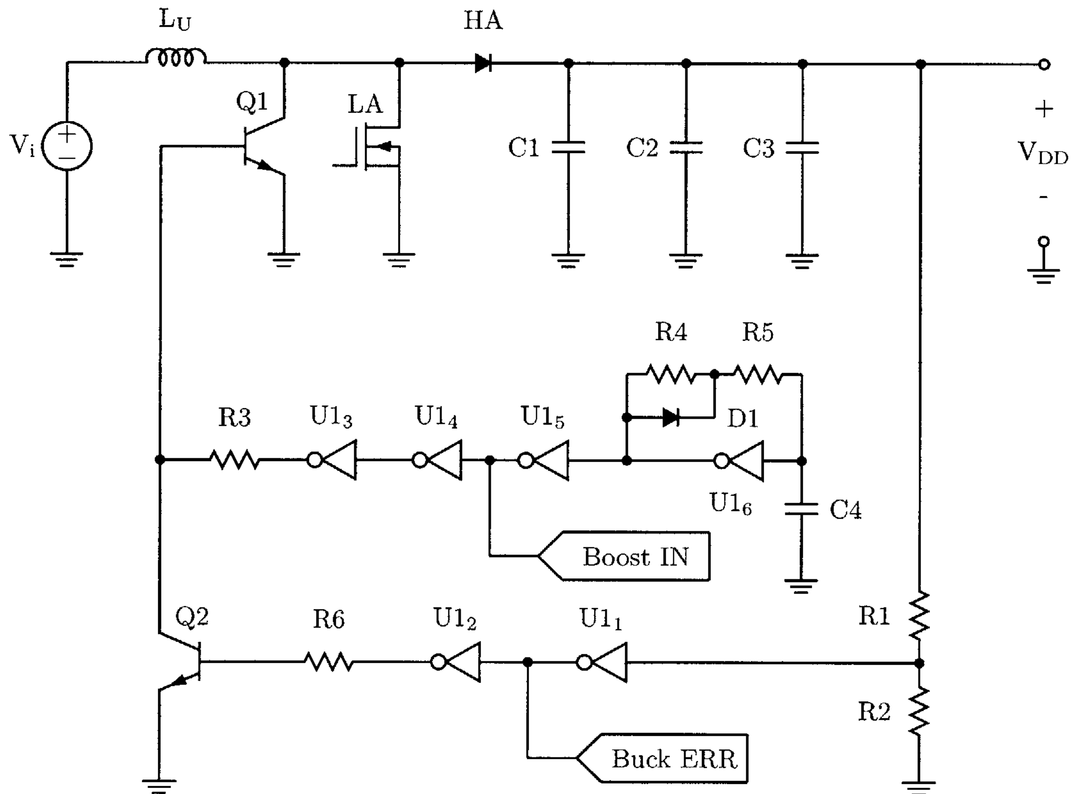

Figure 5.10: Boost stage start-up circuit.

R1:	39k	C1:	2.2μ	D1:	MUR120
R2:	12k	C2:	220μ	D2:	1N4148
R3:	100	C3:	2.2μ		
R4:	12k	C4:	200p	Q1:	40N10
R5:	15k	U1:	74HC14	Q2:	2N2222
R6:	100	L1:	47μ	Q3:	2N4401

Table 5.2: Suggested values for the boost startup circuit.

The circuit is implemented with one 74HC14, and two 2N2222 transistors. Q_1 and LA both operate from a 60% duty ratio square wave oscillating at 250 kHz that is generated by U_{1_6}, R_4, R_5, C_4, and D_1. When the output voltage is too low to operate LA, Q_1 is activated and operates the converter. The output voltage is measured and scaled by the voltage divider created by R_1 and R_2. U_{1_1} disables the buck converter and U_{1_2} activates Q_1 by turning Q_2 off. Once Q_1 raises the boost voltage high enough (after about 10 cycles), the LA driver begins to operate. During this period, Q_1 and LA operate in tandem. After one or two cycles of tandem operation, the boost converter is self-sustaining. The high output voltage turns on the buck converter, and Q_2 disables Q_1. The node labeled "Boost IN" connects the IN of the IR2125 that drives LA. The node labeled "Buck ERR" connects to the ERR shutdown pins of the IR2125s that drive the buck FETs.

Chapter 6

Lab 3: Isolated and Indirect Converters, Resonant Converters

IN this lab, the student designs and builds a high-voltage flyback converter and an electric ballast for a fluorescent lamp [5], [12], [13]. These exercises teach common ways to create a high voltage from a low voltage. A flyback converter also teaches an indirect converter with transformer isolation. Appendix D presents portions of Ken Schrock's final project for 6.131 [9], where he builds a light dimmer that may be added to Lab 3 in future offerings of 6.131.

6.1 Flyback Converter

In this exercise, the student is asked to build a flyback converter with the following specifications, according to the topology shown in Figure 6.1.

Specification	**Value**	**Unit**
Input Voltage:	24	V
Output Voltage:	200	V
Switching Frequency:	100	kHz
Duty ratio:	0.8	
Output Power:	2	W
Min. load CCM:	2	W
Core:	P30/19	3C90-A1000

The design of this converter follows. The conversion ratio for the flyback is

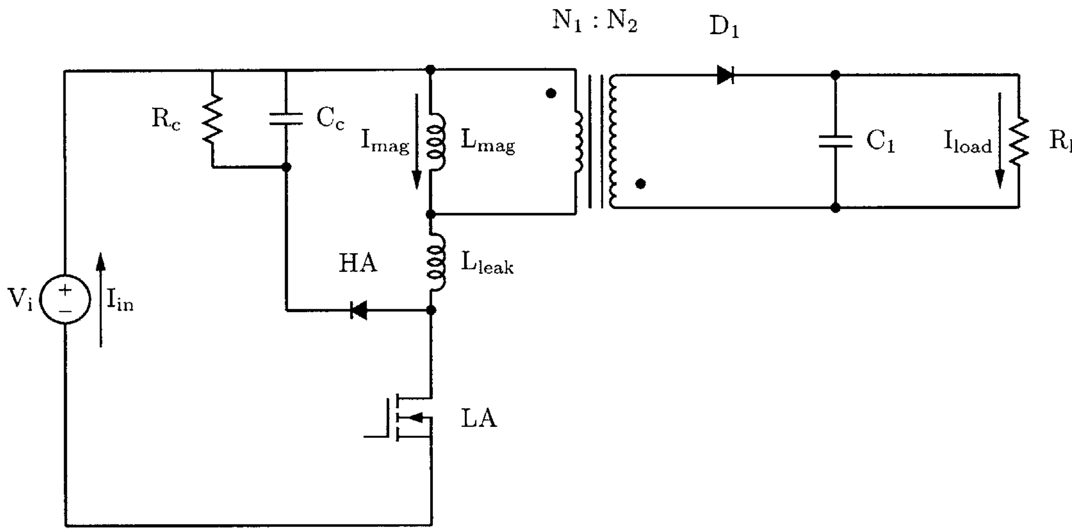

Figure 6.1: The suggested flyback topology.

$$\frac{V_{out}}{V_{in}} = \frac{N_2}{N_1}\frac{D}{1-D} \tag{6.1.1}$$

substituting and solving for the transformer winding ratio yields

$$\frac{200V}{24V} \cdot \frac{.2}{.8} = \frac{N_2}{N_1} = 2.08 \tag{6.1.2}$$

Using an averaged circuit model, and assuming 100% efficiency

$$\langle I_{mag} \rangle = \langle I_{in} \rangle + \langle I_{load} \rangle \frac{N_2}{N_1} \tag{6.1.3}$$

by KCL. Using P=VI to solve $\langle I_{in} \rangle$ and $\langle I_{load} \rangle$

$$\langle I_{mag} \rangle = \frac{P_{out}}{V_{in}} + \frac{P_{out}}{V_{out}}\frac{N_2}{N_1} \tag{6.1.4}$$

and substituting the specified values

$$\langle \mathrm{I_{mag}} \rangle = \frac{2\mathrm{W}}{24\mathrm{V}} + \frac{2\mathrm{W}}{200\mathrm{V}} \cdot 2.08 \tag{6.1.5}$$

yields

$$\langle \mathrm{I_{mag}} \rangle = 100\mathrm{mA} \tag{6.1.6}$$

To ensure CCM operation,

$$\mathrm{L_{mag}} > \frac{\mathrm{V_{in}DT}}{2\langle \mathrm{I_{mag}} \rangle} \tag{6.1.7}$$

and substituting the specified values

$$\mathrm{L_{mag}} > \frac{0.8 \cdot 24\mathrm{V} \cdot 10\mu\mathrm{s}}{2 \cdot 100\mathrm{mA}} \tag{6.1.8}$$

results in

$$\mathrm{L_{mag}} > 960\mu H \tag{6.1.9}$$

The "instructor solution" for this problem uses $\mathrm{L_{mag}} = 1800\mu\mathrm{H}$. As specified, the core used is a P30/19-3C90-A1000 from Ferroxcube, which has an $\mathrm{A_l} = 1000$. Thus the number of turns on the primary and secondary transformer windings are

$$\mathrm{N_l} = \sqrt{\frac{\mathrm{L_{mag}[nH]}}{\mathrm{A_l}}} \tag{6.1.10}$$

substituting

$$= \sqrt{\frac{18 \cdot 10^5 \text{ nH}}{1000 \ \frac{\text{nH}}{\text{turns}^2}}} \tag{6.1.11}$$

indicates that

$$\text{N}_1 = \ 42 \text{ turns} \tag{6.1.12}$$

then using (6.1.2) to solve for N_2

$$\text{N}_2 = \ 87 \text{ turns} \tag{6.1.13}$$

In CCM, the magnitude of the inductor ripple current is

$$\Delta i = \frac{\text{V}_{\text{in}}\text{DT}}{\text{L}_{\text{mag}}} \tag{6.1.14}$$

substituting values yields

$$\Delta i = \frac{24\text{V} \cdot 0.8 \cdot 10\mu\text{s}}{1800\mu\text{H}} \tag{6.1.15}$$

or

$$\Delta i = \ 100\text{mA} \tag{6.1.16}$$

The peak magnetizing current is

$$\text{I}_{\text{peak}} = \langle \text{I}_{\text{mag}} \rangle + \frac{\Delta \text{i}}{2} \tag{6.1.17}$$

substituting the values found in (6.1.6) and (6.1.16)

$$I_{peak} = 150mA \tag{6.1.18}$$

The resistor and capacitor, R_c and C_c, form a clamp that absorbs the energy stored in the transformer leakage inductance. After winding a test transformer, the leakage inductance measured was 8.8 μH. While the clamp is active, the current in the leakage inductance ramps down from I_{peak} to zero. The expression for the leakage current during this time is

$$i_{lk} = \frac{v_{lk}}{L_{lk}} t + I_{peak} \tag{6.1.19}$$

where I_{peak} is the peak value of the magnetizing current just before the FET turns off, and v_{lk} is the voltage applied to the leakage inductance while the FET is off. While the clamp is active, the voltage across the leakage inductance is

$$v_{lk} = (V_{in} + V_o \frac{N_1}{N_2}) - (V_{in} + V_c) \tag{6.1.20}$$

canceling V_{in} simplifies this to

$$v_{lk} = (V_o \frac{N_1}{N_2} - V_c) \tag{6.1.21}$$

where V_c is the voltage on the clamp capacitor. Note that v_{lk} must be negative to discharge the leakage current. In other words

$$V_c > V_o \frac{N_1}{N_2} \tag{6.1.22}$$

Rewriting (6.1.19) at $t = \Delta t$, the time when $i_{lk} = 0$, results in

$$\Delta t = -\frac{I_{peak} L_{lk}}{v_{lk}} \tag{6.1.23}$$

and the average clamp current then is given by integrating (6.1.19) over the switch period and dividing by T

$$\langle i_{clamp} \rangle = \frac{\frac{1}{2} \Delta t I_{peak}}{T} \tag{6.1.24}$$

Substituting (6.1.21) and (6.1.23) into (6.1.24) results in

$$\langle i_{clamp} \rangle = \frac{1}{2} \frac{\frac{L_{lk} I_{peak}^2}{(V_o \frac{N_1}{N_2} - V_c)}}{T} \tag{6.1.25}$$

For example, choosing $V_c = 131V$ results in a 35V clamping potential across the leakage inductance. Substituting values from the table of specifications, (6.1.26) becomes

$$\langle i_{clamp} \rangle = \frac{1}{2} \frac{8.8\mu H \cdot (150mA)^2}{10\mu s \cdot (96V - 131V)} \tag{6.1.26}$$

which yields

$$\langle i_{clamp} \rangle = 280\mu A \tag{6.1.27}$$

Since the potential across the clamp is 131V, the power delivered to the clamp is

$$P_{clamp} = \langle i_{clamp} \rangle V_{clamp} \tag{6.1.28}$$

and substituting in the appropriate values yields

$$P_{clamp} = 280\mu A \cdot 131V \tag{6.1.29}$$

or

$$P_{clamp} = 36.7\text{mW} \tag{6.1.30}$$

To find a suitable value for the clamp resistance, the power dissipated in the resistor is

$$\frac{V_{clamp}^2}{R_{clamp}} = P_{clamp} \tag{6.1.31}$$

P_{clamp} is given by 6.1.30 and $V_{clamp} = 131\text{V}$, so

$$R_{clamp} = \frac{(131\text{V})^2}{36.7\text{mW}} \tag{6.1.32}$$

which yields

$$R_{clamp} = 467\text{k}\Omega \tag{6.1.33}$$

6.2 Resonant Converter

Next the students design and analyze a resonant converter that can strike and continuously operate a fluorescent lamp. They use their go-kart circuit to drive this resonant lamp ballast. A fluorescent lamp produces light when an electrical arc excites mercury gas within a nearly evacuated glass tube. Ultraviolet light is emitted from the excited gas which, in turn, is absorbed by a white phosphor coating on the inside of the tube. When bombarded with UV, the phosphor fluoresces and illuminates. An unlit lamp presents a high impedance load and about 300V is needed to arc through the tube to ionize the trace gas inside. Once that voltage is applied and the lamp strikes the electrical characteristics of the lamp change. First, its impedance drops to relatively low levels, but secondly the incremental impedance is *negative.* This occurs because as more current flows through the mercury gas, more gas is ionized, which generates more charge carriers — thus increasing its conductivity. To maintain a higher current you must lower the voltage and vice versa, as seen in a typical VI-characteristic for a fluorescent lamp, shown if Figure 6.2. A lit lamp has an incremental impedance of approximately -100Ω.

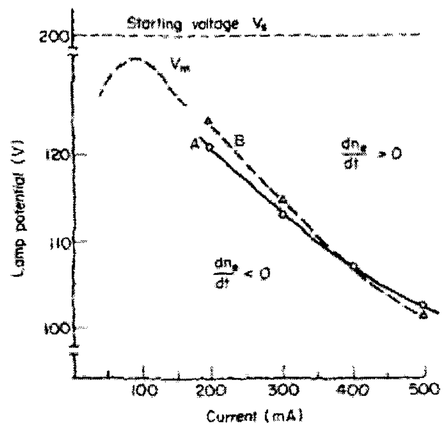

Figure 6.2: A typical V-I characteristic of a fluorescent lamp. [11]

Due to the negative impedance of a lit lamp, care must be taken when designing a ballast, as the operating point of the lamp may not be stable. Assume, for instance, that a lamp is functioning at some operating point along its VI curve. Now if the voltage is fixed but the current is perturbed slightly, perhaps it increases due to temperature fluctuation, then the number of charge carriers increases which causes the current to increase, and so on.

Therefore to illuminate the lamp the ballast must generate an initial high voltage to strike the lamp, and then maintain a stable operating point. A typical fluorescent lamp ballast that can fulfill these requirements is shown in Figure 6.3. The unlit lamp looks like an open-circuit and therefore the LC tank can have high Q. If operated near resonance, the tank produces a high voltage that strikes the lamp. Once struck, the lamp impedance drops, damping the tank. If the combined impedance of the LC tank plus lit lamp is positive, then the driving circuit sees regular resistive load and operates normally.

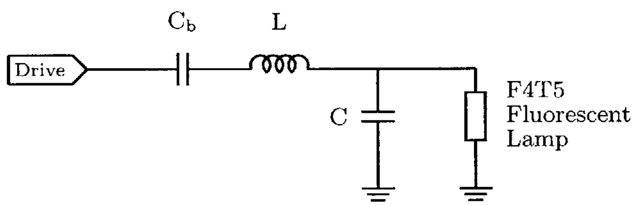

Figure 6.3: Fluorescent lamp ballast.

The student designs two ballasts: one with a powder-iron core, and the other with a ferrite core. The drive voltage is a 40V square wave at 35 kHz. The impedance of the lamp ballast is

$$\frac{V_{out}}{V_{in}}(s) = \frac{R_c Cs + 1}{LCs^2 + (R_c + R_L)Cs + 1} \tag{6.2.1}$$

where R_c and R_L are the effective series resistance of the capacitor and inductor, respectively. The student is also instructed to design using a 22nF 400V capacitor. They investigate two candidate cores, a P30/19-3C90-A1000 ferrite core and T106-52 iron-powder core. For each design they are to estimate the magnitude of the resonant peak to ascertain which core is the best, lowest loss choice. The resonant frequency of the LC tank, assuming lightly damped operation, is

$$f = \frac{1}{2\pi\sqrt{LC}} \tag{6.2.2}$$

rearranging (6.2.2) to solve for L results in

$$L = \frac{1}{(2\pi f)^2 C} \tag{6.2.3}$$

substituting the specified values

$$L = \frac{1}{(2\pi \cdot 35\text{kHz})^2 \cdot 22\text{nF}} \tag{6.2.4}$$

or

$$L = 0.94 \text{ mH} \tag{6.2.5}$$

For the P30/19-3C90-A1000, $A_l = 1000$. Thus the number of turns needed is,

$$N = \sqrt{\frac{L[\text{nH}]}{A_l}} \tag{6.2.6}$$

substituting the appropriate values

$$N = \sqrt{\frac{940 \cdot 10^3 \text{ nH}}{1000 \frac{\text{nH}}{\text{turns}^2}}} \tag{6.2.7}$$

results in

$$N = 31 \text{ turns} \tag{6.2.8}$$

$$\tag{6.2.9}$$

Next, to estimate the current in L, it is assumed that the output voltage amplitude is 400V and that the lamp has not yet struck. Therefore, the inductor current is

$$I = \frac{V}{\frac{1}{Cs}} \tag{6.2.10}$$

which these values

$$I = 400 \cdot 2\pi \cdot 35\text{kHz} \cdot 22\text{nF} \tag{6.2.11}$$

results in

$$I = 1.91\text{A} \tag{6.2.12}$$

peak-to-peak current. The RMS inductor current then in

$$I_{rms} = 1.35\text{A} \tag{6.2.13}$$

The peak flux density for this core with an effective area $A_e = 1.37\ \text{cm}^2$,

$$B_{pk} = \frac{V_{rms} \cdot 10^8}{4.44 A_e N f} \tag{6.2.14}$$

with the appropriate values

$$B_{pk} = \frac{\frac{400}{\sqrt{2}} \cdot 10^8}{4.44 \cdot 1.37\ \text{cm}^2 \cdot 31\ \text{turns} \cdot 35\ \text{kHz}} \tag{6.2.15}$$

yields

$$B_{pk} = 4333\ \text{gauss} \tag{6.2.16}$$

The core loss associated with an AC flux of this magnitude to be $P_v = 700\ \frac{\text{kW}}{\text{m}^3}$ for this core. The volume of the core is $V_e = 6190\text{mm}^3$, therefore the power dissipated in the core is $6190\ \text{mm}^3 \cdot 10^{-6} \cdot 700\ \frac{\text{kW}}{\text{m}^3} = 4.33\ \text{W}$. To estimate R_L,

$$R_L = \frac{P}{I_{rms}^2} \tag{6.2.17}$$

substituting the values for the power loss and RMS current

$$R_L = \frac{4.33 \text{ W}}{(1.35 \text{ A})^2} \tag{6.2.18}$$

gives

$$R_L = 2.37\ \Omega \tag{6.2.19}$$

Using (6.2.1), and assuming $R_c = 2\ \Omega$, then the magnitude of the resonant peak is 33.

Repeating these steps for the T106-51 core yields the following results:

Result	**Value**	**Unit**
A_L	95	$\frac{nH}{turn^2}$
A_e	0.659	cm^2
V_e	4.28	cm^3
N	100	turns
B_{pk}	2777	gauss
P_v	5500	$\frac{kW}{m^3}$
P	23.5	W
R_L	12.7	Ω

These values correspond to an LC tank with a resonant magnitude of 12.

Based on these results, the student sees that the ferrite core results in a less damped resonant circuit. They build and test their lamp ballast with each core. With the T106-52, the lamps do not strike — the core losses too great; with the P30/19-3C90-A1000 core the lamp strikes and operates reliably.

Chapter 7

Lab 4: DC to AC

IN this lab, the student learns about two types of electric machines, the induction machine and the permanent magnet machine, and how to drive them [6]. A special teaching motor, shown in Figure 7.1, for use in 6.131 [10]. This machine can be configured as either an induction or permanent magnet machine.

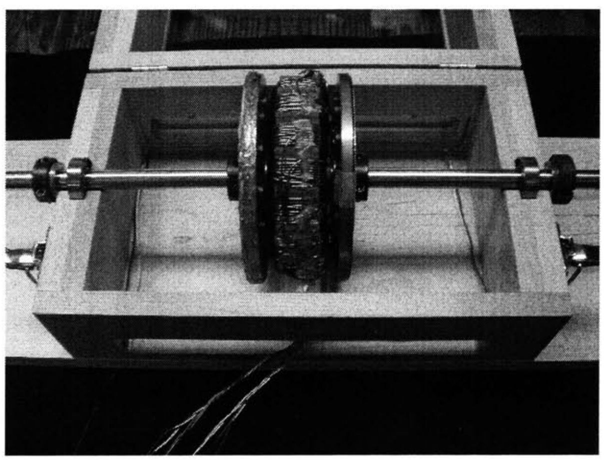

Figure 7.1: The 6.131 Teaching Motor.

A rotor disk for the machine is shown in Figure 7.2. Rare earth magnets are attached in an alternating pattern around the disk. The reverse side of the disk is clad in copper; this side faces the stator when the machine is operated as an induction machine. To function as a permanent magnet machine, it is necessary for the power electronics to know the position of the shaft. An encoder wheel, with the pattern shown in Figure 7.3, is used to signal the power electronics appropriately. This pattern is sensed by a sensor board, shown in Figure 7.4, designed by Warit Wichakool.

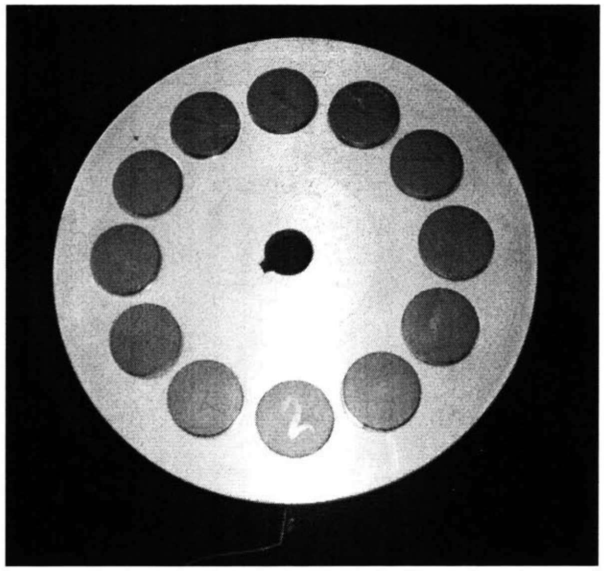

Figure 7.2: The permanent magnet disk.

7.1 Three Phase Permanent Magnet Machine

A block diagram of the operation of the permanent magnet machine is shown in Figure 7.5. The position of the rotor is feed back to a state machine that keeps track of which MOSFETs to turn on and off. The state machine is shown in Figure 7.6. The encoder wheel has two tracks: a count track, and a reset track. The count track increments the 74LS163, and thus the state of the machine. The reset signal is positioned at every sixth count signal. The six states are decoded by a 74LS138 multiplexor. The group of NAND gates produce a six pulse excitation pattern. Note that the high side signals are gated with three AND gates so that a PWM signal can be used to control the speed on the induction machine.

7.2 Three Phase Induction Machine

For the induction machine they build a state machine that activates the six MOSFETs to produce a "six pulse" sinusoid approximation. This circuit is shown in Figure 7.7.

The state machine is similar to the state machine for the permanent magnet motor, however,

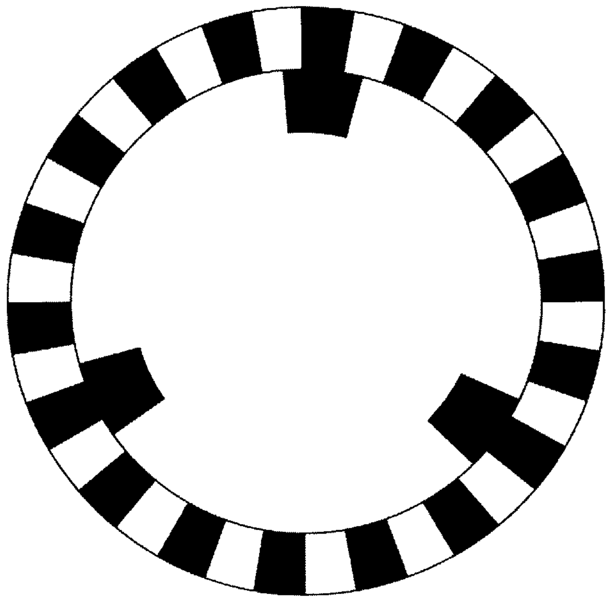

Figure 7.3: The encoder wheel pattern.

this state machine is free running. An external oscillator signals a state change by incrementing the 74LS163 counter, and the sixth line of the multiplexor is used to reset the counter.

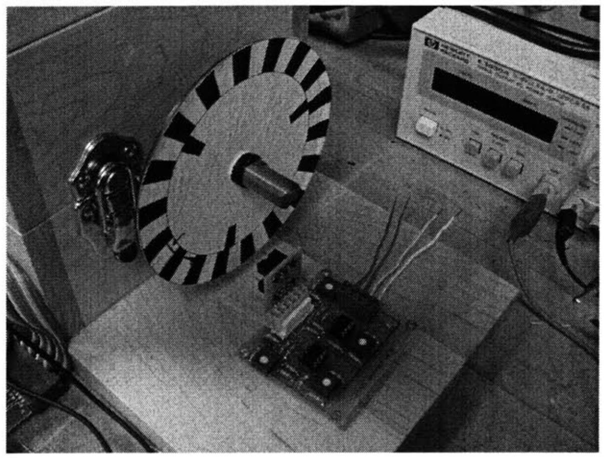

Figure 7.4: The encoder wheel for the permanent magnet machine.

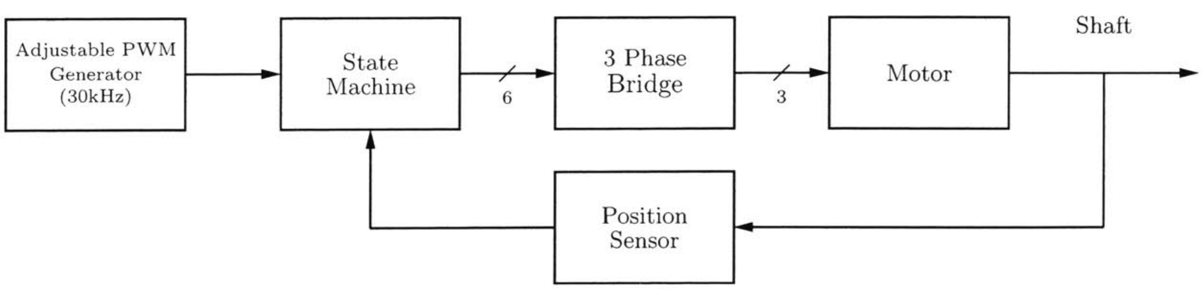

Figure 7.5: Block diagram for the permanent magnet machine.

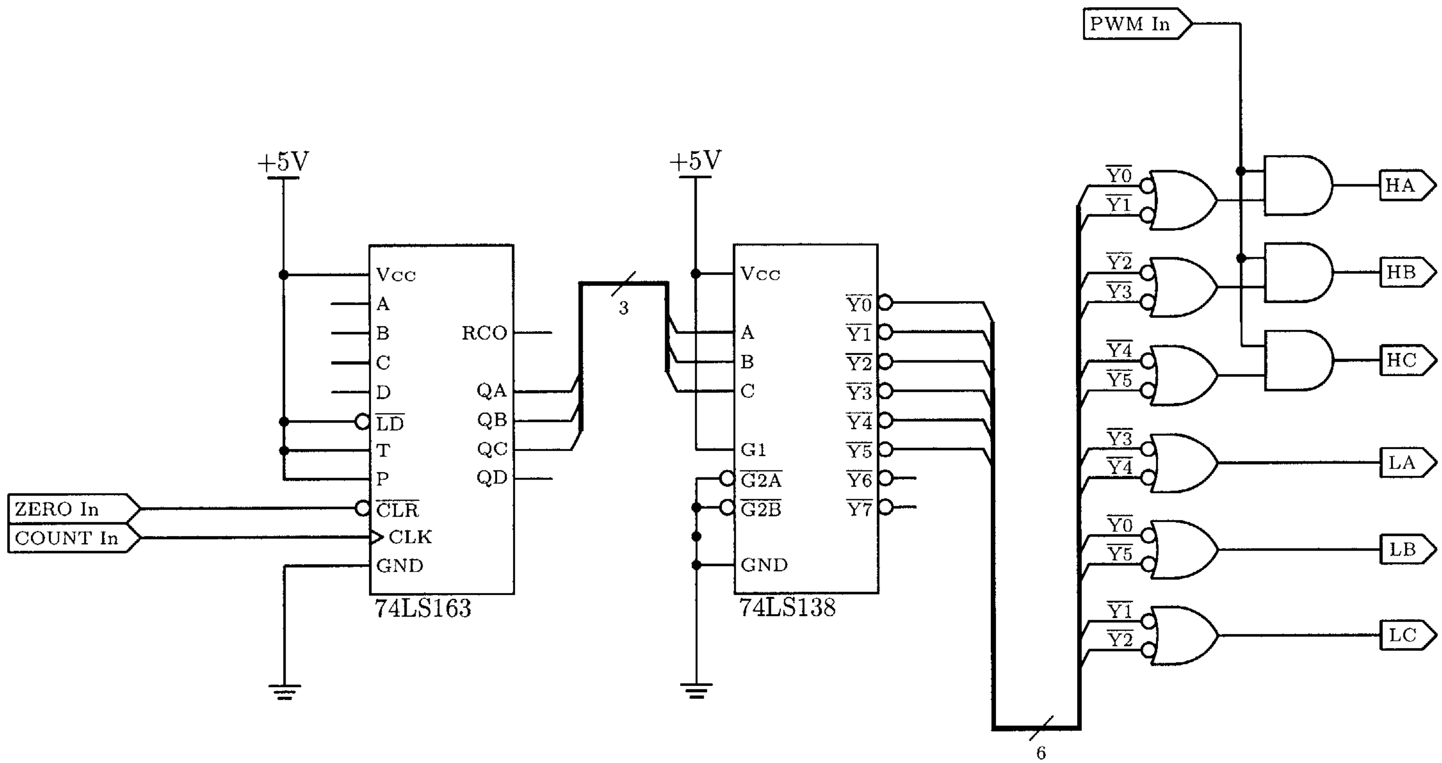

Figure 7.6: The state machine used to control the PM machine.

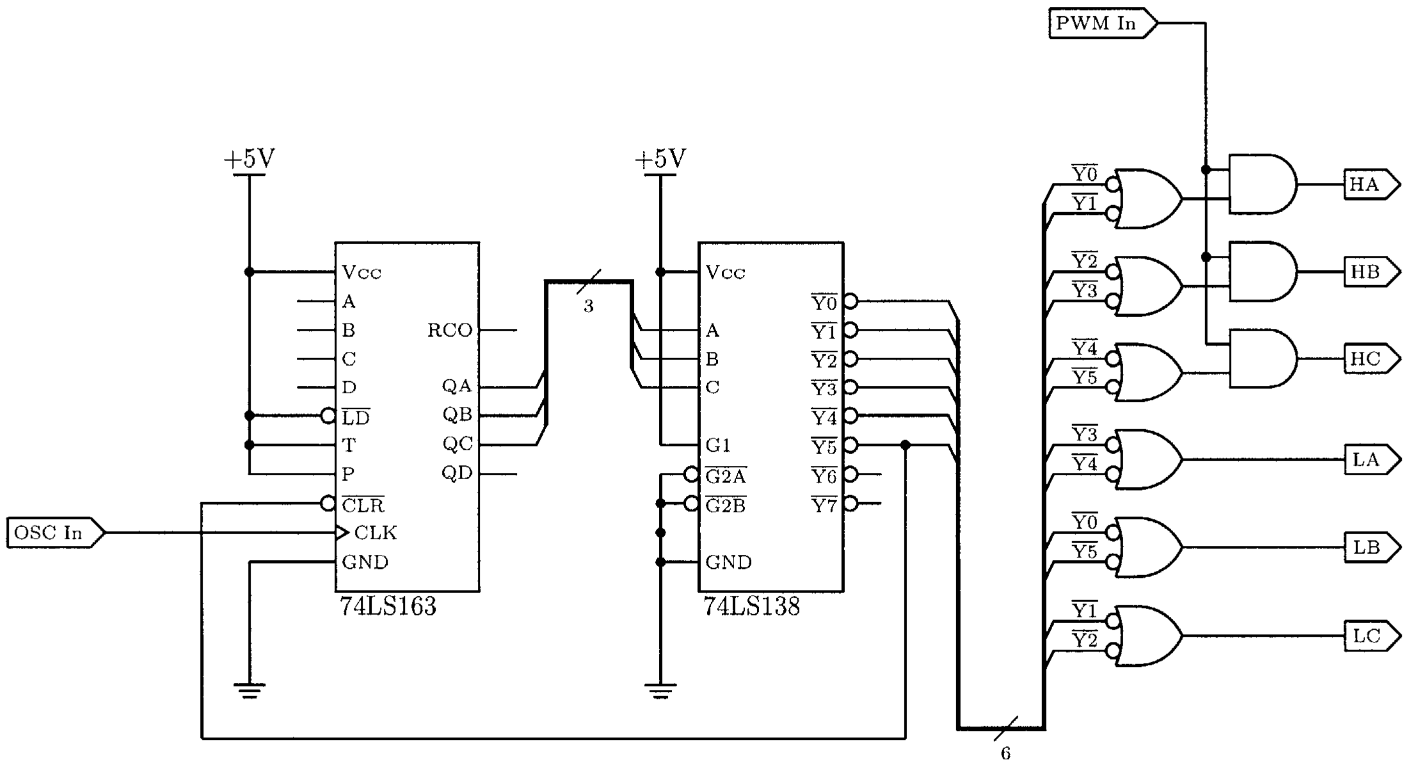

Figure 7.7: A state machine to produce "six pulse" sinusoidal excitation.

Chapter 8

Assessment and Conclusion

TO a large degree, the material in this class is self-assessing: if the exercise is designed correctly and properly built, then it works; otherwise, it does not. As 6.131 is design oriented, laboratory checkoffs and demonstrations are used in the course to assess the student's mastery of the material. This assessment begins during a scheduled design review, where the student sits with a staff member and walks through their design analysis. It ends with a laboratory demonstration at a live checkoff with a staff member.

The design review is a 60 minute mandatory discussion with a staff member. The goal of the review is two-fold: first, to correct any mistakes before the student begins to build, and second to assign a grade based on the merit of their design. The first purpose is crucial as hours and hours can be wasted building a poorly designed system; help at a judicious point in the process minimizes frustration and aides in learning. The staff members are instructed to make sure that each student leaves the review with a good design so that they are not penalized for it later. Once the student understands the material, they are given the parts they need to build the lab.

At the review, the student is shown a grading sheet such as the Lab 2 sheet shown in Figure 8.1. The student is expected to come prepared with a thorough understanding of the lab, and with full schematics: including a layout diagram for each circuit using the laminated cards in Appendix B. The student is expected to follow a design process similar to that presented in Chapters 5 and 6. During the Lab 2 design review, for instance, the student explains how they designed two inductors and two capacitors to meet specifications. In the Lab 3 review, the student presents their design for the flyback transformer and clamp. Each topic of the review is judged as excellent, good, acceptable, and needs improvement. In general, receiving mostly "goods" and a few "excellents" is enough to earn all the points for a design review. The acceptable column is for students who made a good attempt at the topic, but ultimately had a serious flaw that would prevent operation. Notice that we mean "acceptable" in the sense that their understanding of the material is "acceptable" but not necessarily their design. The "needs improvement" category is for the student who comes to the review unprepared.

The course staff is available, throughout the entire process, during open office hours. The available hours are posted weekly, and scheduled so that staff help is available every day, even if only for one hour. More hours are scheduled preceding design reviews and laboratory checkoffs.

The second component of the laboratory grade, which is the result of a 15 minute demonstration with a staff member. At the checkoff, the student demonstrates to the staff member the circuitry they built for the exercises. After the circuit is visually checked and operated, points are assigned based on the completeness and functionality of the circuitry.

The final two grades come from a comprehensive quiz, given after all the labs have been completed, and from the final project. The final project is on a topic of the student's choosing. The student and the staff work together through a series of interviews to establish the scope for the project and to establish reasonable outcomes. The final projects are assessed by the staff based on the metrics and goals developed during the final project interviews. A typical final project, provided by Ken Schrock, is included as Appendix D. For his project, Ken constructed a digital phase-controller to modulate the brightness of incandescent lamps. As a further step, he used a series of band-pass filters to flash a bank of lamps along with music.

The first offering of the class was a success, based on the student reviews of the course, as summarized by Eta Kappa Nu below, [1]

> *"Four design projects constituted the heart of this class, with everything else designed to supplement them. Each lab required a design review, where students could go over proposed designs with the course staff before beginning to implement their ideas. Most found the labs well laid-out and appreciated the emphasis on design and debugging. The labs were very helpful in demonstrating the theory presented in lecture, and were essential to understanding the material. The equipment and support was great, but the design projects were extremely time consuming."*

"Fun, practical lab experience"

"Good equipment"

Hands-on learning is critically valuable in an engineering education. This thesis presents the tools and exercises that solve some of the problems that arise when teaching power electronics through hands-on experiences. The labs and equipment presented here have been designed to bring instructors and students together in learning, in an exciting, fostering, and safe environment.

STUDENT: STAFF MEMBER:

6.188 CHECK-LIST for LAB 2 DESIGN REVIEW:

	EXCELLENT!	GOOD	ACCEPTABLE	PLEASE IMPROVE BEFORE NEXT DR
DESIGN CRITERIA (Below) ↓	Knowledgable, thoughtfully designed, selected, and or explained (1.5 points each)	Clear effort with possible errors but leading to a rich, thoughtful discussion during review. (1 point each)	Some effort, significant errors, conversant in course topics, left the DR after staff discussions with a plan for building. (0.5 points each)	Unprepared; insufficient knowledge of the lab material to be confident of successful design after DR (0 points each)
Stereo Buck Inductor Selection				
Stereo Buck Capacitor Selection				
Stereo Boost Inductor Selection				
Stereo Boost Capacitor Selection				
Topological layout on totem card for boost and buck converter (laminate sheet)				
Understanding and presentation of control circuitry for buck/boost and for the boost "bootstrap" circuit.				
Other issues as appropriate that arise during review (comment:)				

Grade plan:

- Place a check mark in the appropriate place for each design criterion.
- Sum all points.
- Saturate total score at 7.5 points (full credit). That is, it is possible to "score" more than 7.5 points. Only 7.5 points will be awarded for "full credit".

TOTAL SCORE (MAX of 7.5): ____________

Figure 8.1: Design review grade sheet used to assess each student's design work in Lab 2.

Appendix A

Manufacturing Information for the PowerNerd Kit

A.1 Power NerdKit Part and Vendor Information

Part Number	Vendor	Description	Quantity
	J&J	Card Cage	1
	J&J	Power Cage	1
92060A220	McMaster-Carr	Captive Screws	4
15145A61	McMaster-Carr	Alum. Pull Handle, 6" center, #8-32	2
90273A146	McMaster-Carr	#6-32x3/8" screw, IEC screw (pack of 100)	2
90675A007	McMaster-Carr	#6-32 nut w/tooth washer, IEC nut	2
90403A194	McMaster-Carr	#8-32x1/2 screw for fastening power cage	14
90675A009	McMaster-Carr	#8-32 nut w/lock ring, powercage and fan	12
90126A011	McMaster-Carr	Power Cage washers #10-32 3/64	16
90403A201	McMaster-Carr	Fan Screws #8-32 x 1 3/8	4
104432	Jameco	PS connector	2
104715	Jameco	PS connector	2
103915EC	Jameco	fuse 2A fast GMA	1
174140	Jameco	12VDC Fan	1
148689	Jameco	MeanWell dual supply +12, -12	1
212353	Jameco	MeanWell single supply +5	1
199523	Jameco	30VDC line transformer	1
208346	Jameco	Y-type power cord	1
78318	Jameco	PS crimp lugs	6
102832	Jameco	Fuse Holder	1
H781-ND	Digikey	Mscrew Alum 4-40 3/8	16
1808K-ND	Digikey	Standoff Hex Alum .625	8
WM18232-ND	Digikey	Battery spade connectors 16AWG	4
2221K-ND	Digikey	Standoff Hex Alum 2" 8-32	6
0701RBY	Electronix	Binding Post, Blue	2
0701RB	Electronix	Binding Post, Black	2
0701RY	Electronix	Binding Post, Yellow	2
0701RR	Electronix	Binding Post, Red	1
0701RG	Electronix	Binding Post, Green	1
44F7570	Newark	Battery	2
81N1649	Newark	Cardguides	28
98F1819	Newark	Double Stick tape	1
03F1911	Newark	16 AWG wire, Red	1
03F1913	Newark	16 AWG wire, Yellow	1
03F1914	Newark	16 AWG wire, Green	1
03F1917	Newark	16 AWG wire, White	1
03F1918	Newark	16 AWG wire, Black	1
03F1919	Newark	16 AWG wire, Blue	1
95F7500	Newark	1/8 heatshrink tubing	1
PB-400	All Electronics	Breadboard	3
STS-42	All Electronics	SPDT on-off-on switch	1
STS-8	All Electronics	DPDT on-off-on switch	1
SPH-386	All Electronics	IEC	1
FHP-28	All Electronics	ATC fuse holder	2
FSA-3	All Electronics	3A ATC fuse	1

Vendor	Contact Person	Phone Number	Specialty
J & J fabricators	John Matthews	781-899-2373	Lab Kit Fabrication
Proxy	Shawn D. Foy	978-687-3138	Box Build and Circuit Fabrication
McMaster-Carr		mcmaster.com	Parts
Jameco		jameco.com	Parts
Digi-Key		digikey.com	Parts
All Electronics		allelectronics.com	Parts
Electronix		electronix.com	Parts

A.2 Power NerdKit Card-Cage Drawings

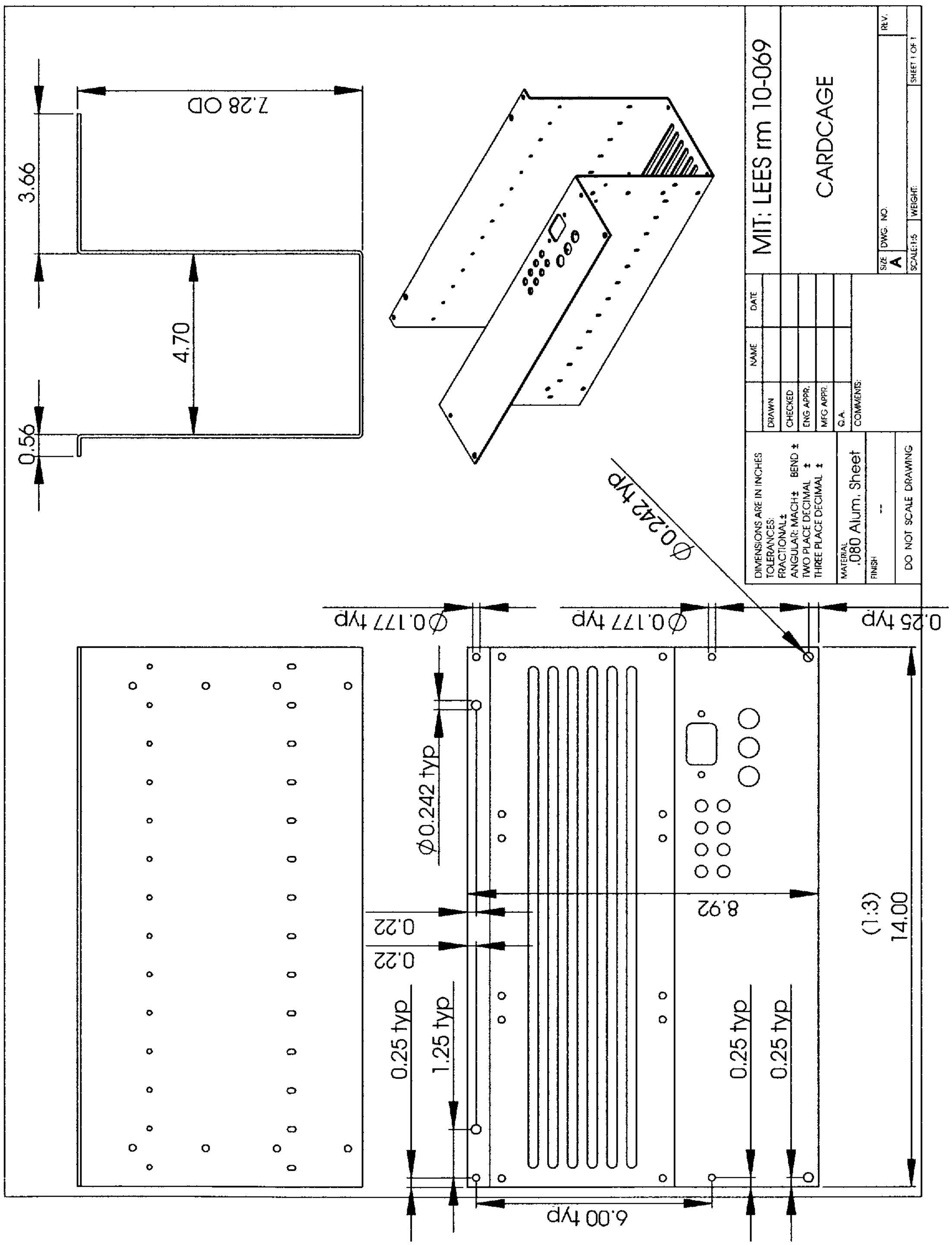

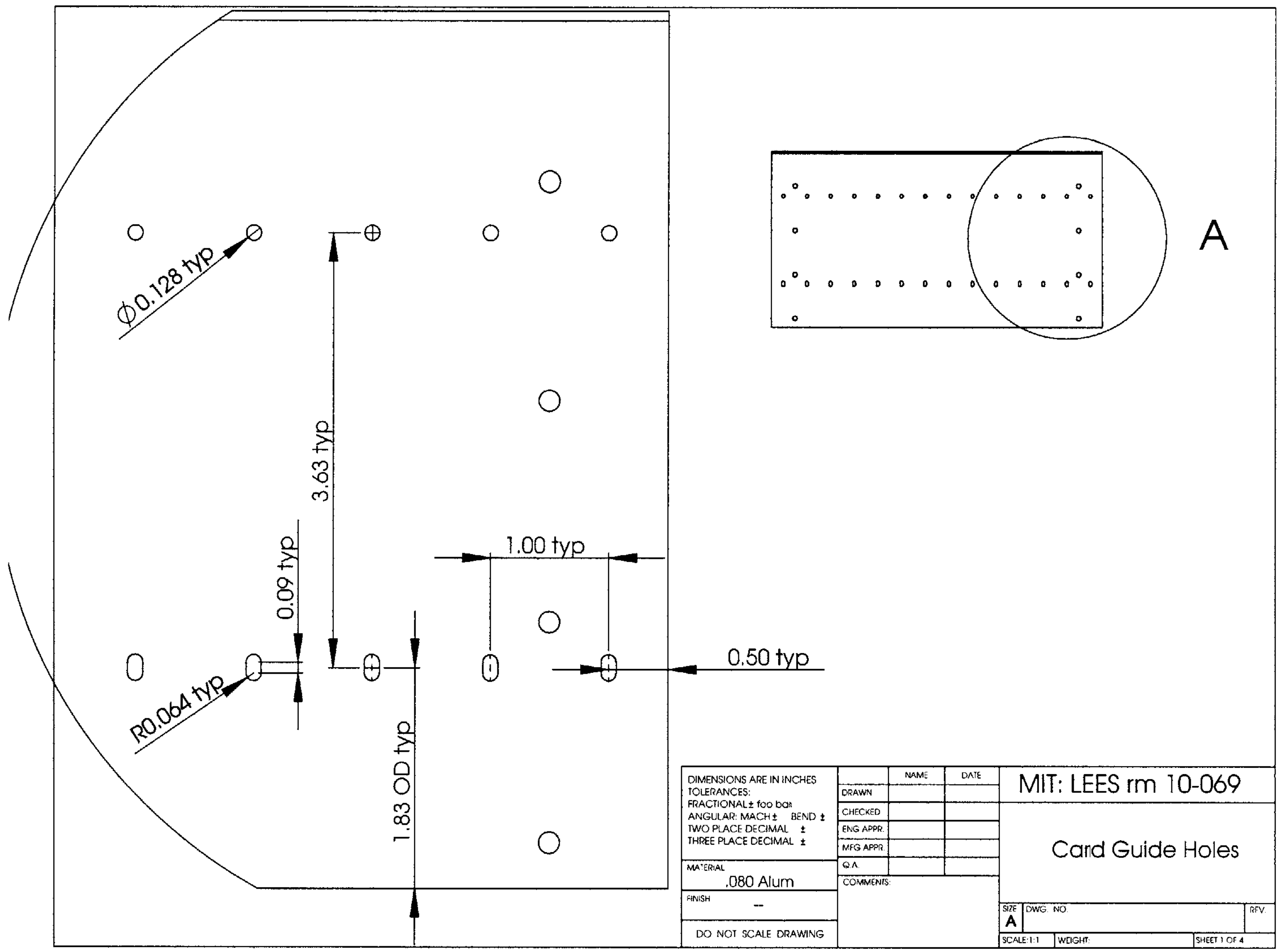

ϕ0.128 typ
3.63 typ
0.09 typ
1.00 typ
0.50 typ
R0.064 typ
1.83 OD typ
A
DIMENSIONS ARE IN INCHES
TOLERANCES:
FRACTIONAL ± foo bar
ANGULAR: MACH ± BEND ±
TWO PLACE DECIMAL ±
THREE PLACE DECIMAL ±
MATERIAL
.080 Alum
FINISH
--
DO NOT SCALE DRAWING
NAME
DATE
DRAWN
CHECKED
ENG APPR.
MFG APPR.
Q.A.
COMMENTS:
MIT: LEES rm 10-069
Card Guide Holes
SIZE
A
DWG. NO.
REV.
SCALE: 1:1
WEIGHT:
SHEET 1 OF 4

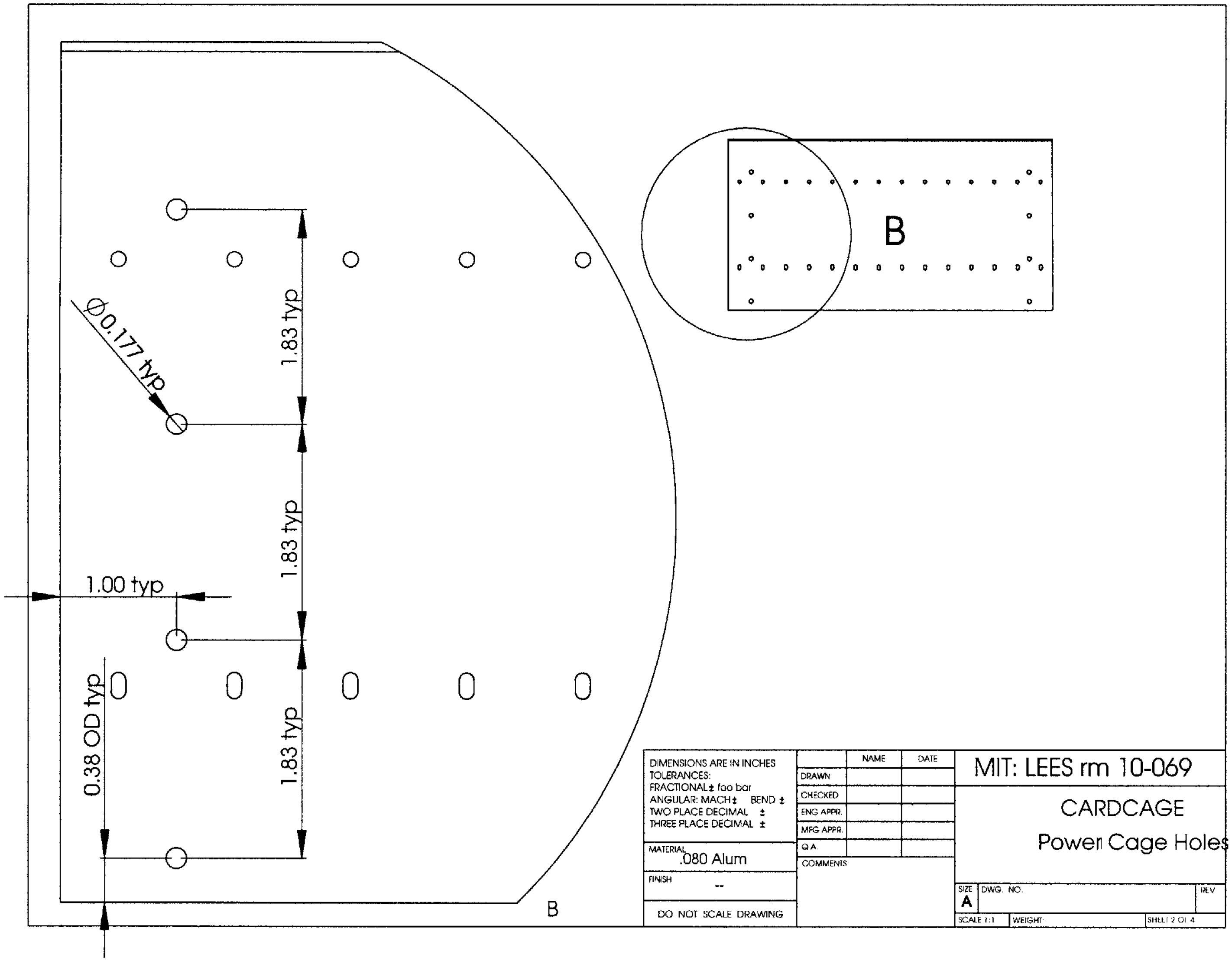
Ø0.177 typ
1.83 typ
1.83 typ
1.83 typ
1.00 typ
0.38 OD typ
B
B
DIMENSIONS ARE IN INCHES
TOLERANCES:
FRACTIONAL± foo bar
ANGULAR: MACH± BEND ±
TWO PLACE DECIMAL ±
THREE PLACE DECIMAL ±
MATERIAL .080 Alum
FINISH --
DO NOT SCALE DRAWING
NAME
DATE
DRAWN
CHECKED
ENG APPR.
MFG APPR.
Q.A.
COMMENTS
MIT: LEES rm 10-069
CARDCAGE
Power Cage Holes
SIZE A
DWG. NO.
REV
SCALE 1:1
WEIGHT
SHEET 2 OF 4

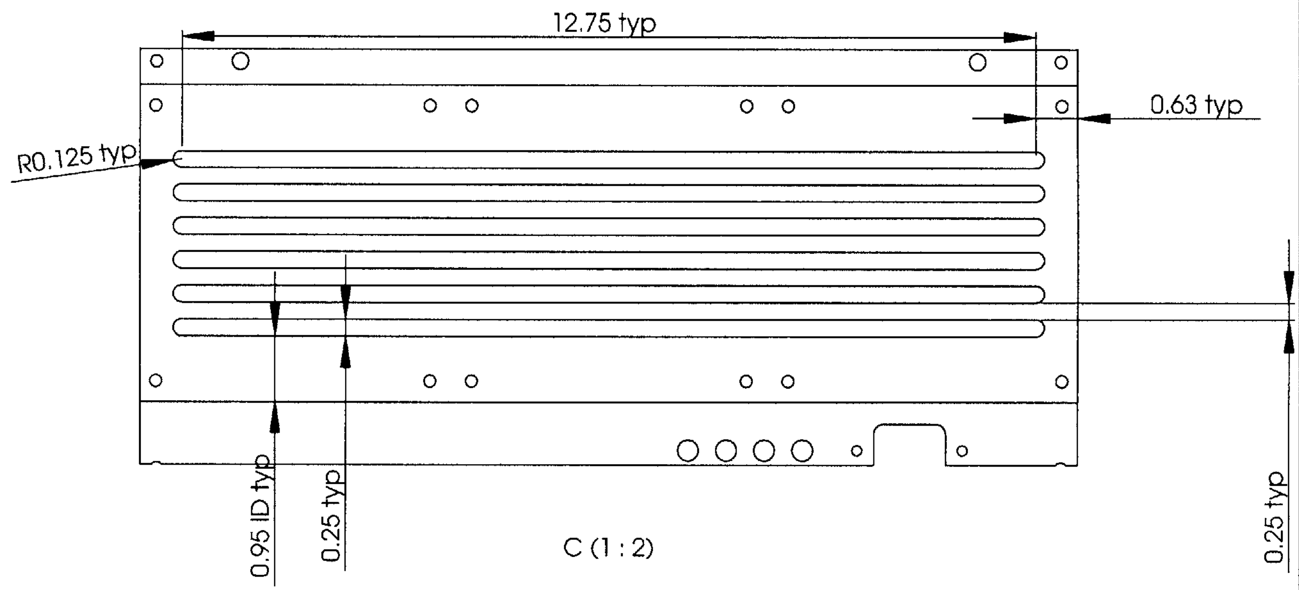

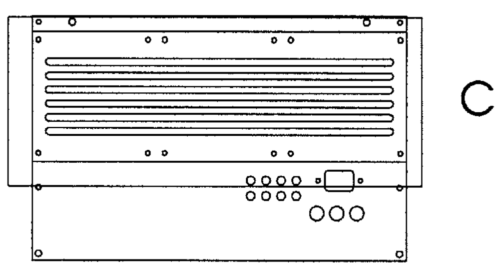

DIMENSIONS ARE IN INCHES
TOLERANCES:
FRACTIONAL± foo bar
ANGULAR: MACH± BEND ±
TWO PLACE DECIMAL ±
THREE PLACE DECIMAL ±

MATERIAL .080 Alum

FINISH --

DO NOT SCALE DRAWING

	NAME	DATE
DRAWN		
CHECKED		
ENG APPR.		
MFG APPR.		
Q.A.		

COMMENTS:

MIT: LEES rm 10-069

Fan Slots

SIZE A DWG. NO. REV

SCALE 1:2 WEIGHT: SHEET 3 OF 4

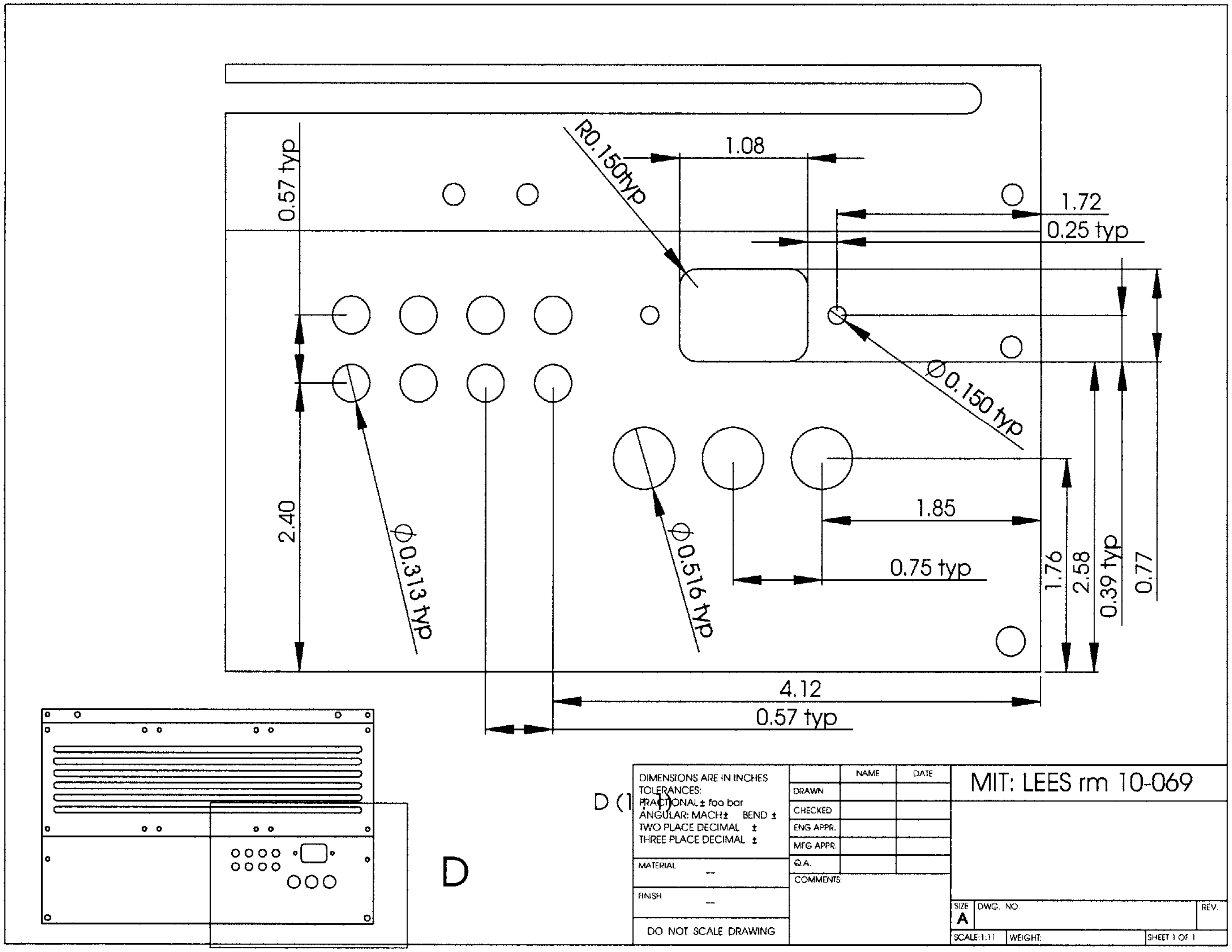

R0.150typ
1.08
0.57 typ
1.72
0.25 typ
Φ0.150 typ
2.40
Φ0.313 typ
Φ0.516 typ
1.85
0.75 typ
1.76
2.58
0.39 typ
0.77
4.12
0.57 typ
D (1 : 1)
D
DIMENSIONS ARE IN INCHES
TOLERANCES:
FRACTIONAL ± foo bar
ANGULAR: MACH ± BEND ±
TWO PLACE DECIMAL ±
THREE PLACE DECIMAL ±
MATERIAL --
FINISH --
DO NOT SCALE DRAWING
NAME
DATE
DRAWN
CHECKED
ENG APPR.
MFG APPR.
Q.A.
COMMENTS:
MIT: LEES rm 10-069
SIZE A
DWG. NO.
REV.
SCALE: 1:11
WEIGHT:
SHEET 1 OF 1

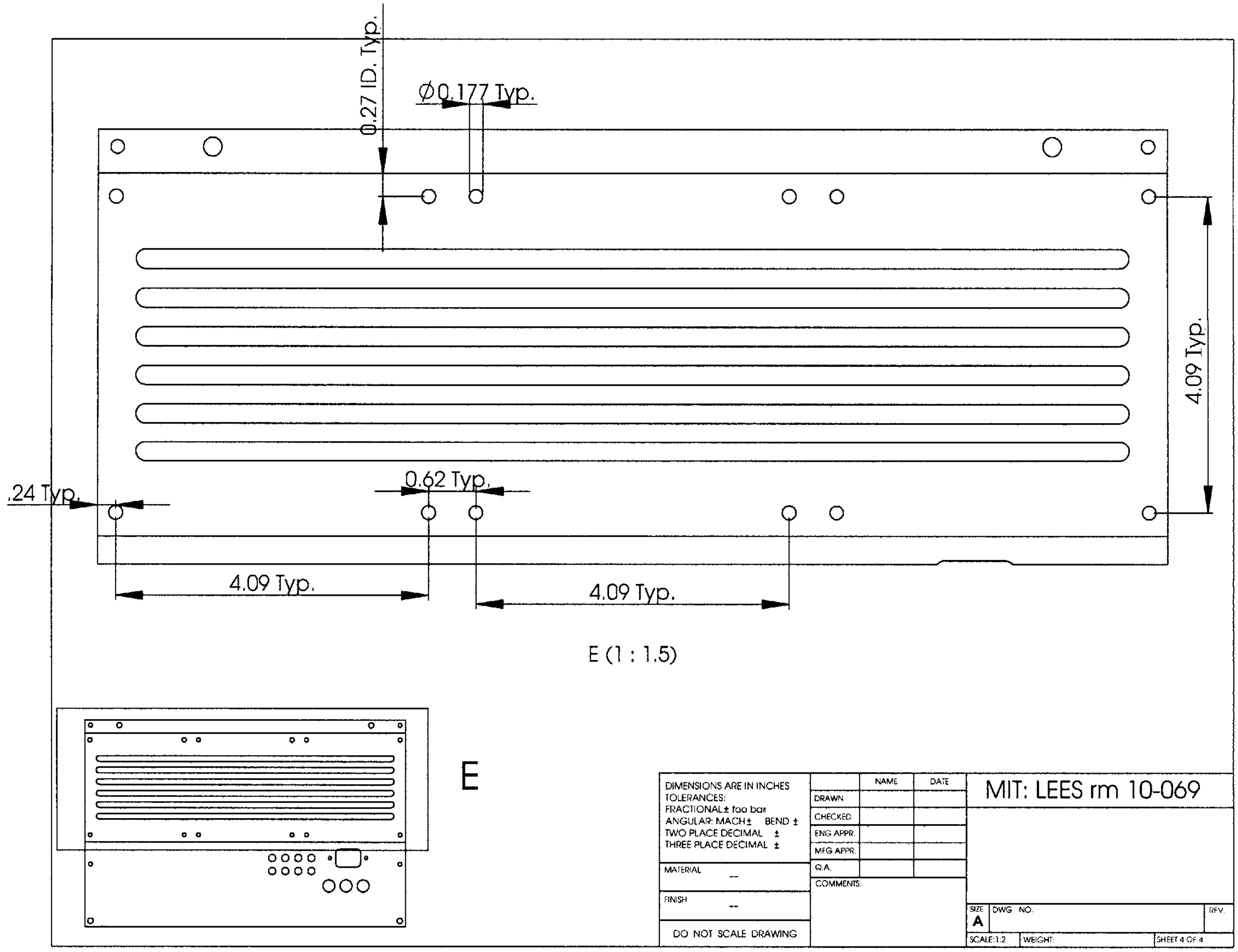
0.27 ID. Typ.
Ø0.177 Typ.
4.09 Typ.
.24 Typ.
0.62 Typ.
4.09 Typ.
4.09 Typ.
E (1 : 1.5)
E
DIMENSIONS ARE IN INCHES
TOLERANCES:
FRACTIONAL± foo bar
ANGULAR: MACH± BEND ±
TWO PLACE DECIMAL ±
THREE PLACE DECIMAL ±
MATERIAL
--
FINISH
--
DO NOT SCALE DRAWING
NAME
DATE
DRAWN
CHECKED
ENG APPR.
MFG APPR.
Q.A.
COMMENTS:
MIT: LEES rm 10-069
SIZE
A
DWG NO.
REV.
SCALE:1:2
WEIGHT:
SHEET 4 OF 4

A.3 Power NerdKit Power-Cage Drawings

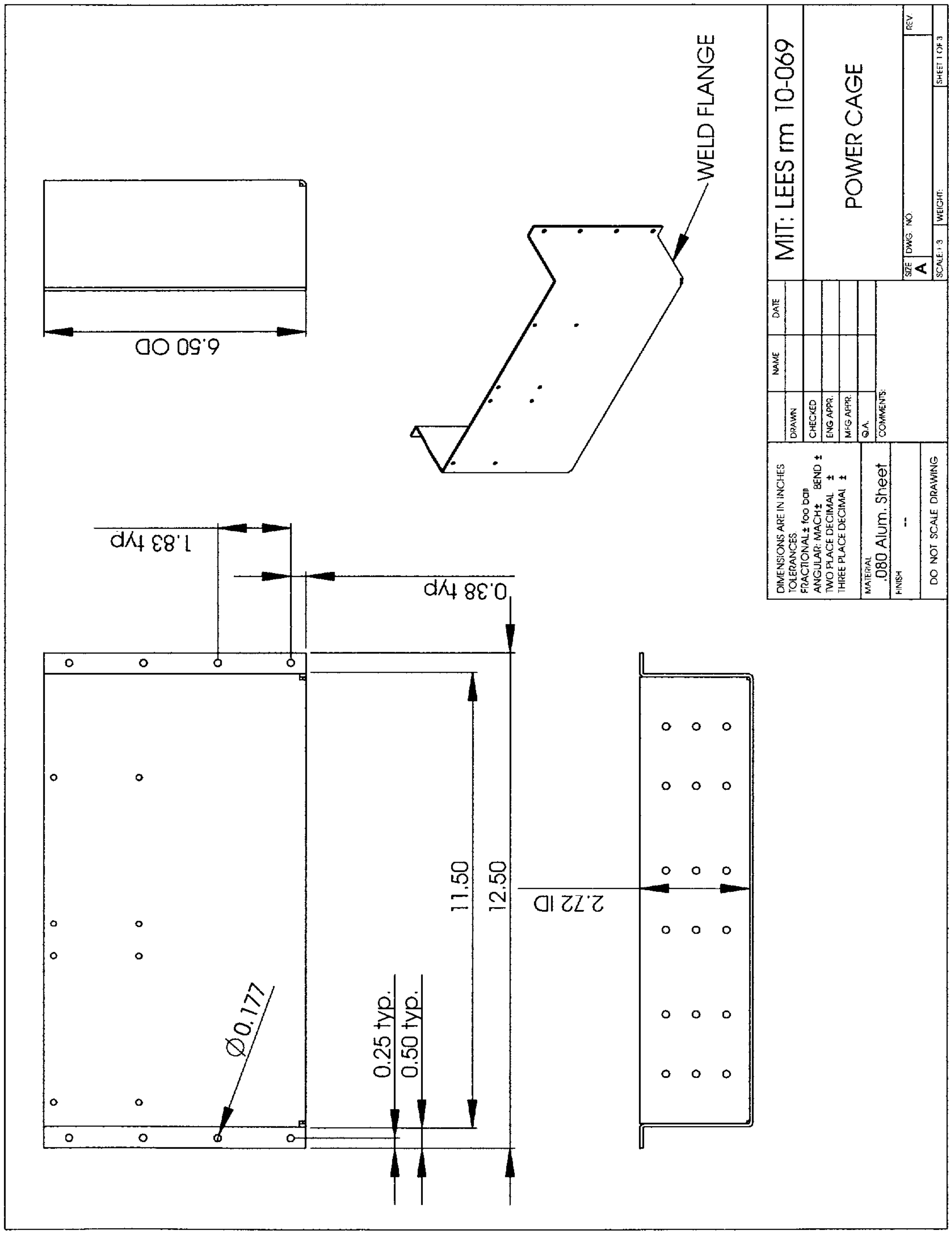

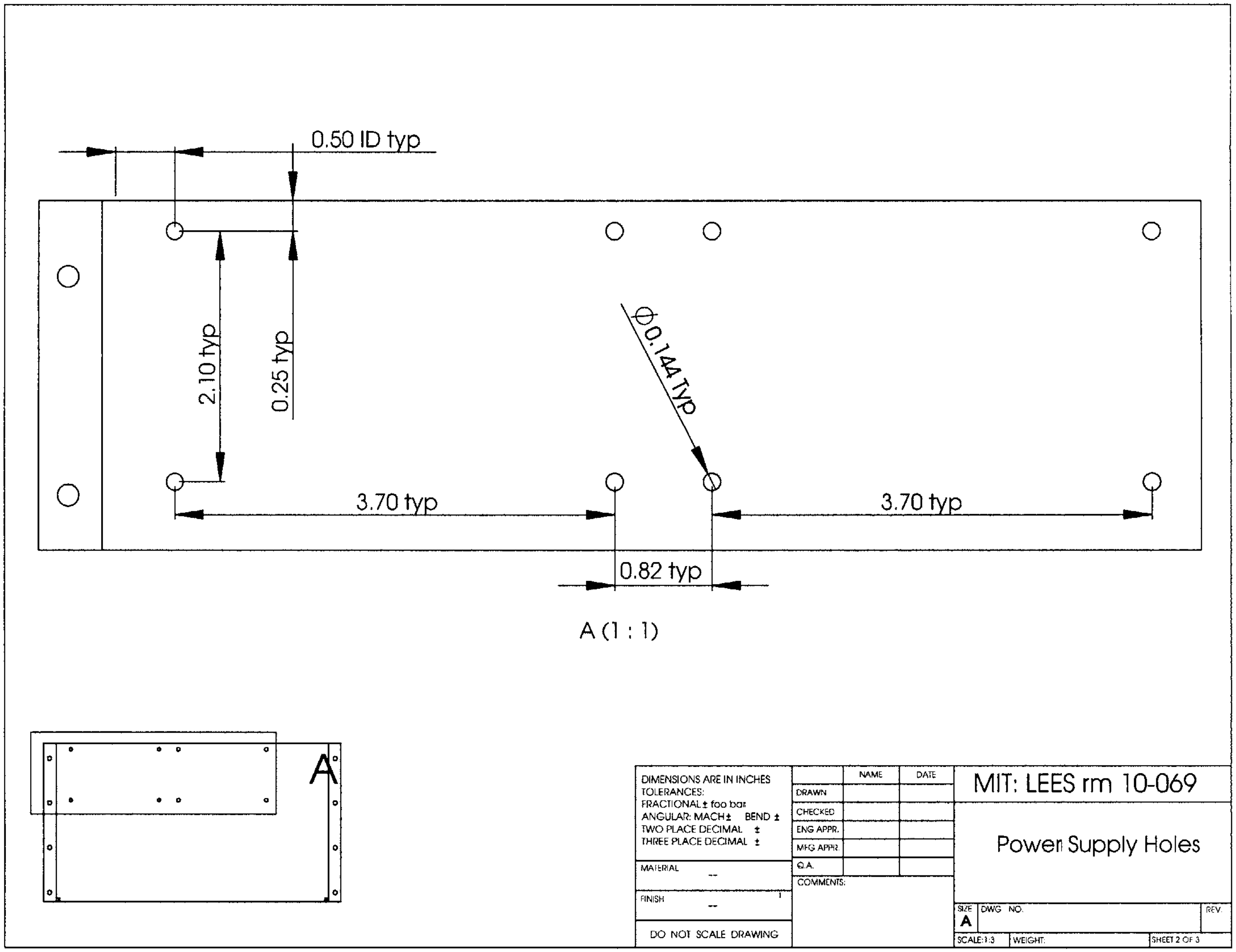
0.50 ID typ
2.10 typ
0.25 typ
Ø0.144 Typ
3.70 typ
3.70 typ
0.82 typ
A (1 : 1)
A
DIMENSIONS ARE IN INCHES
TOLERANCES:
FRACTIONAL ± foo bar
ANGULAR: MACH ± BEND ±
TWO PLACE DECIMAL ±
THREE PLACE DECIMAL ±
MATERIAL --
FINISH --
DO NOT SCALE DRAWING
NAME
DATE
DRAWN
CHECKED
ENG APPR.
MFG APPR.
Q.A.
COMMENTS:
MIT: LEES rm 10-069
Power Supply Holes
SIZE A
DWG. NO.
REV.
SCALE: 1:3
WEIGHT:
SHEET 2 OF 3

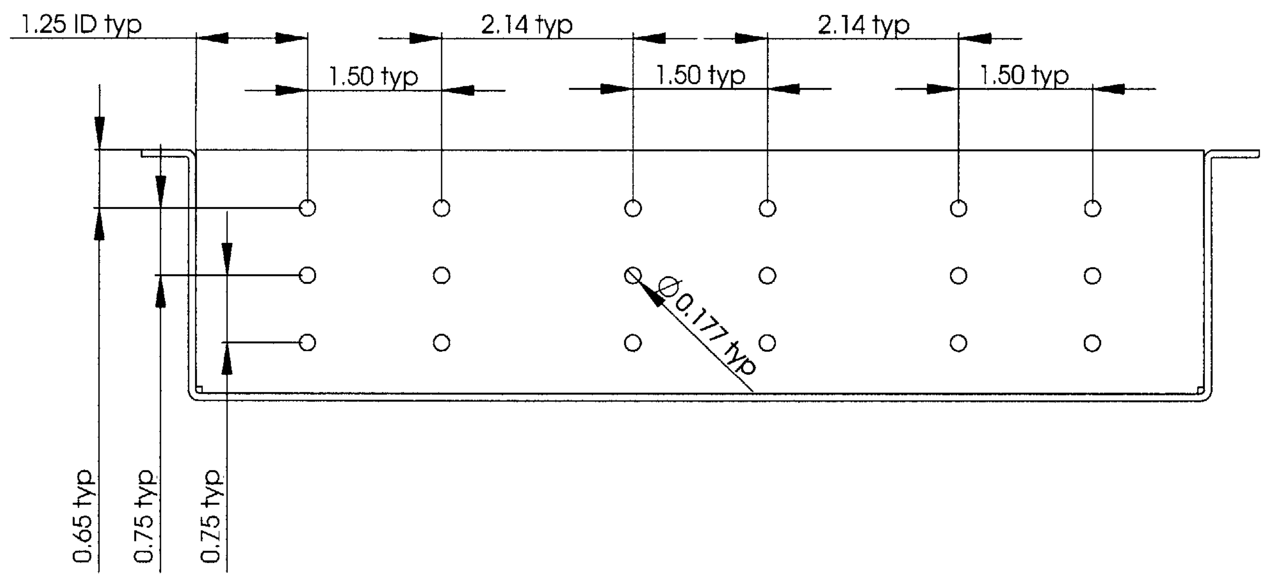

DIMENSIONS ARE IN INCHES
TOLERANCES:
FRACTIONAL ± foo bar
ANGULAR: MACH ± BEND ±
TWO PLACE DECIMAL ±
THREE PLACE DECIMAL ±

MATERIAL --

FINISH --

DO NOT SCALE DRAWING

	NAME	DATE
DRAWN		
CHECKED		
ENG APPR.		
MFG APPR.		
Q.A.		

COMMENTS:

MIT: LEES rm 10-069

Power Cage Bottom Holes

SIZE A | DWG. NO. | REV.

SCALE: 1:3 | WEIGHT: | SHEET 3 OF 3

Appendix B

Layout Cards

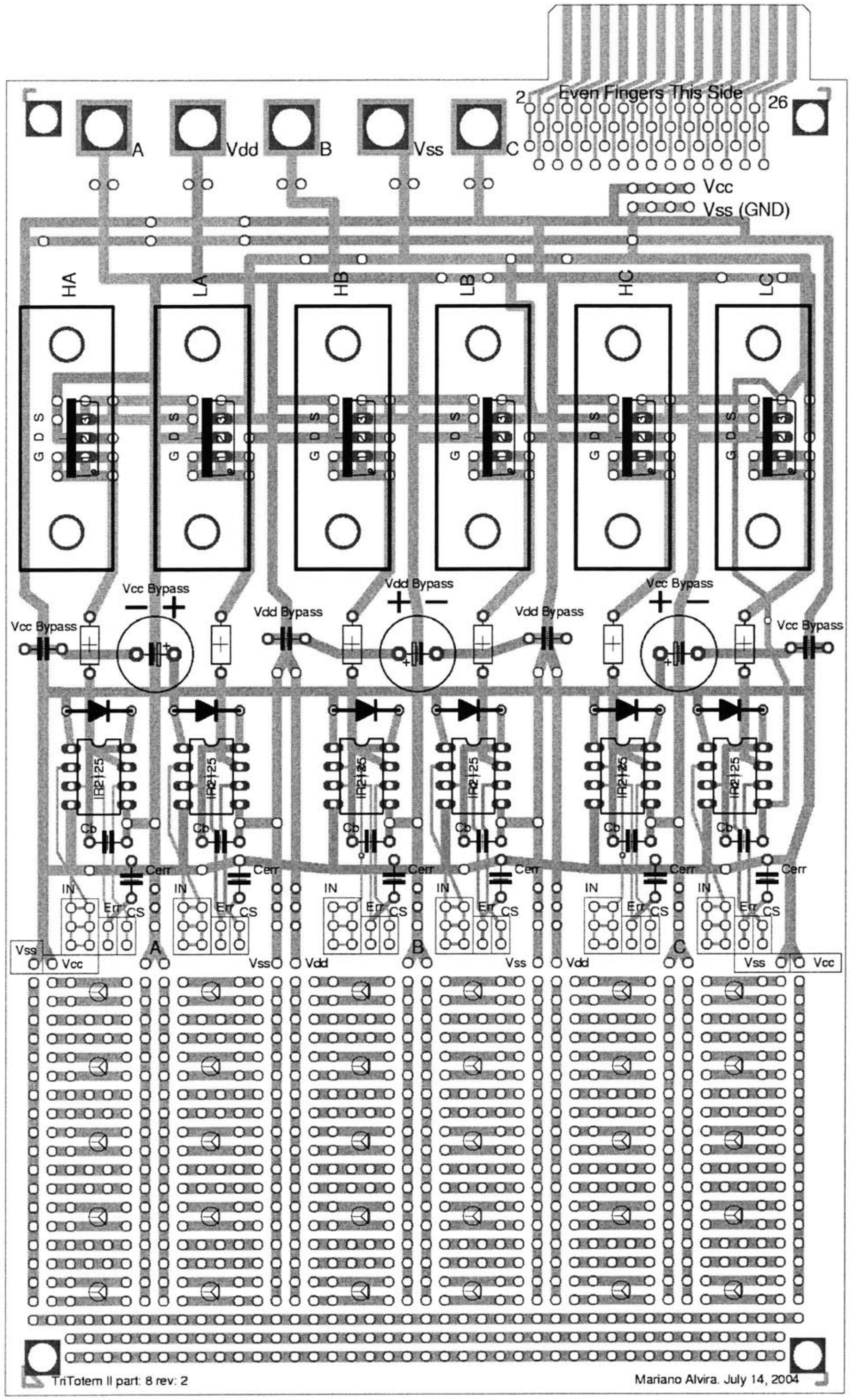

Figure B.1: The laminated design sheet for the TriTotem II Card.

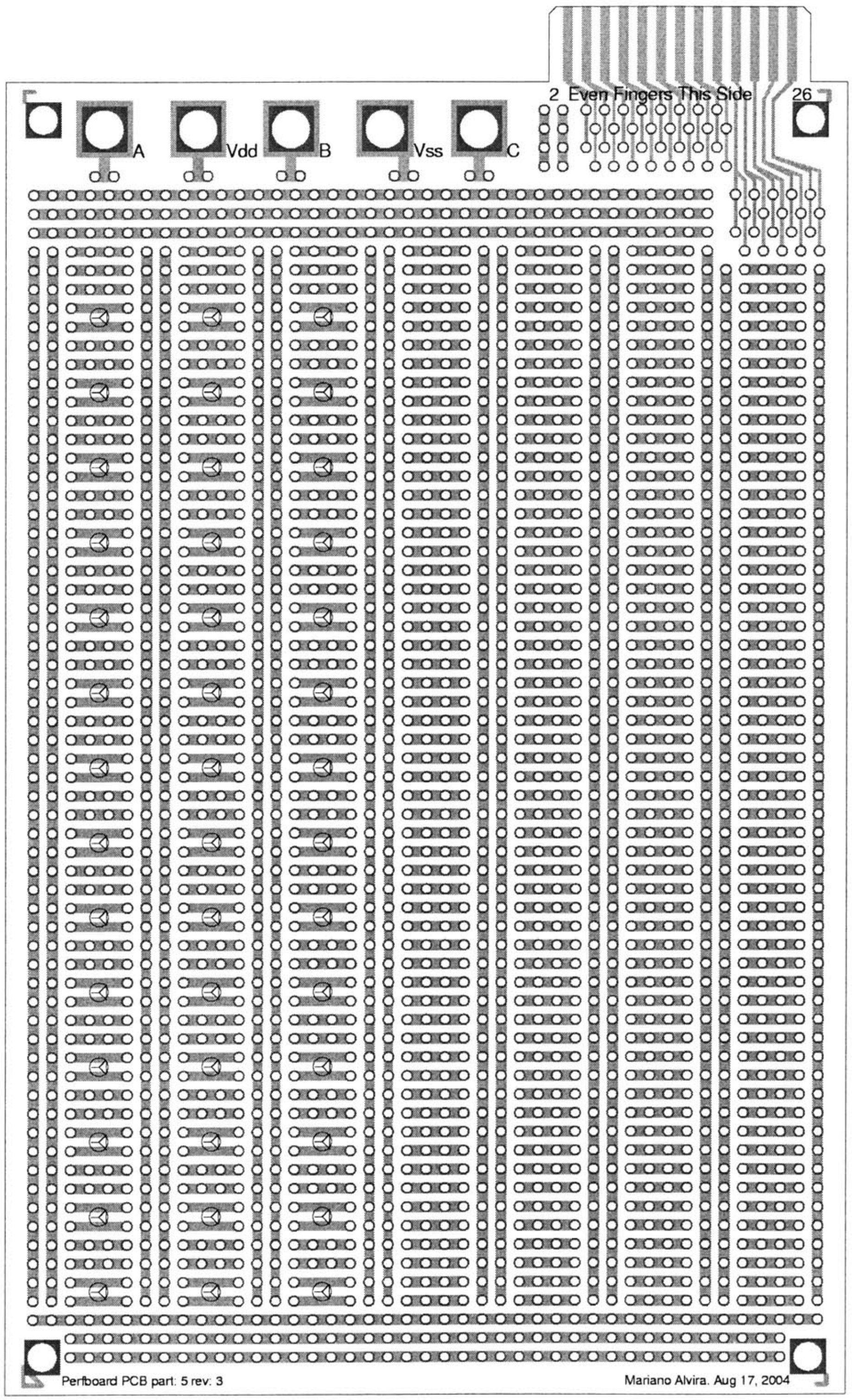

Figure B.2: The laminated design sheet for the Solder Card.

Appendix C

Parametric Inductor Saturation Code

```
H = 20 % Mag. Force for 20% mu derating -26 material
H52 = 25 % Mag. Force for 20% mu derating -52 material
% from Micrometals databook

core1 = ["-@1;T-20-26;"; "-@2;T-26-26;"; "-@3;T-30-26;";\
 "-@4;T-37-26;"; "-@5;T-38-26;"];
core2 = ["-@1;T-44-26;"; "-@2;T-50-26;"; "-@3;T-50-26B;"];
core3 = ["-@1;T-51-26C;"; "-@2;T-60-26;"; "-@3;T-68-26;"; "-@4;T-80-26;"];
core4 = ["-@1;E-49-26;" ;"-@2;E-75-26;"; "-@3;E-100-26;"];
core5 = ["-@1;T-225-26;" ;"-@2;T-250-26;";\
 "-@3;T-300-26;"; "-@4;T-400-26;"];
core6 = ["-@1;E-220-26;" ;"-@2;E-305-26;"; "-@3;E-450-26;"];
core7 = ["-@1;T-72-26;"; "-@2;T-90-26;"; "-@3;T-94-26;";\
 "-@4;T-106-26;"; "-@5;T-131-26;"];
core8 = ["-@1;T-150-26;"; "-@2;T-157-26;"];
core9 = ["-@1;T-80-52;"; "-@2;T-106-52;"];
core10 = ["-@1;T-90-52;"; "-@2;T-106-52;"; "-@3;T-131-52;";\
 "-@4;T-157-52;"; "-@5;T-175-52;"];

lm1 = [1.15, 1.47, 1.84, 2.31, 2.18];
lm2 = [2.68, 3.19, 3.19];
lm3 = [2.79, 3.74, 4.23, 5.14];
lm4 = [2.86, 4.20, 5.08];
lm5 = [14.6, 15, 19.8, 25];
lm6 = [13.2, 18.5, 22.9];
lm7 = [4.01, 5.78, 5.97, 6.49, 7.72];
lm8 = [9.38, 10.1];
lm9 = [3.74, 6.49];
lm10 = [5.78, 6.49, 7.72, 10.1, 11.2];

Al1 = [18.5, 57, 33.5, 28.5, 49];
Al2 = [37, 33, 43.5];
Al3 = [83, 50, 43.5, 46];
Al4 = [38, 64, 92];
Al5 = [98, 242, 80, 131];
Al6 = [286, 287, 550];
Al7 = [90, 70, 60, 93, 116];
Al8 = [96, 100];
Al9 = [42, 95];
Al10 = [64, 95, 108, 99, 105];

```

```
maxturns1 = [11, 15, 25, 37, 31];
maxturns2 = [43, 59, 59];
maxturns3 = [36, 67, 74, 103];
maxturns4 = [109, 239, 350];
%maxturns5 = [305, 270, 422, 494];
maxturns5 = [100, 100, 100, 100];


%Real maxturns
%maxturns6 = [1780, 3523, 5511];
%Pretty maxturns
maxturns6 = [1780, 2500, 1000];

%maxturns7 = [54, 115, 117, 118, 134];
maxturns7 = [54, 60, 60, 60, 60];
maxturns8 = [180, 204];
maxturns9 = [103, 118];
maxturns10 = [40, 40, 40, 40, 40];

hold off
figure
for i = 1:length(lm1)
   N = linspace(1, maxturns1(i), maxturns1(i));
   % see pg. 10
   I = (H * lm1(i))./(0.4*pi*N);
   % see pg. 2
   L = (Al1(i) * N.^2) * (10^(-9));
   plot(L,I,core1(i,:))
   hold on
end
title('Starting at 1 turn to max single layer turns at 28 awg')
xlabel(' Nominal Inductance [H]')
ylabel(' I [A] of %80 permeability')

gset terminal postscript
gset output "core.ps"
gset output "/dev/null"
gset terminal x11

hold off
figure
for i = 1:length(lm2)
   N = linspace(20, maxturns2(i), maxturns2(i)-20);
   % see pg. 10
   I = (H * lm2(i))./(0.4*pi*N);
   % see pg. 2
   L = (Al2(i) * N.^2) * (10^(-9));
   plot(L,I,core2(i,:))
   hold on
end
title('Starting at 20 turns to max single layer turns at 28 awg')
xlabel(' Nominal Inductance [H]')
ylabel(' I [A] of %80 permeability')
```

```
gset output "core2.ps"
gset terminal postscript
gset output "/dev/null"
gset terminal x11

hold off
figure
for i = 1:length(lm3)
   N = linspace(20, maxturns3(i), maxturns3(i)-20);
   % see pg. 10
   I = (H * lm3(i))./(0.4*pi*N);
   % see pg. 2
   L = (Al3(i) * N.^2) * (10^(-9));
   plot(L,I,core3(i,:))
   hold on
end
title('Starting at 20 turns to max single layer turns at 28 awg')
xlabel(' Nominal Inductance [H]')
ylabel(' I [A] of %80 permeability')

gset output "core3.ps"
gset terminal postscript
gset output "/dev/null"
gset terminal x11

hold off
figure
%for i = 1:length(lm4)
for i = 1:1
   N = linspace(20, maxturns4(i), maxturns4(i)-20);
   % see pg. 10
   I = (H * lm4(i))./(0.4*pi*N);
   % see pg. 2
   L = (Al4(i) * N.^2) * (10^(-9));
   plot(L,I,core4(i,:))
   hold on
end
title('Starting at 20 turns to max single layer turns at 28 awg')
xlabel(' Nominal Inductance [H]')
ylabel(' I [A] of %80 permeability')

gset output "core4.ps"
gset terminal postscript
gset output "/dev/null"
gset terminal x11

hold off
figure
for i = 1:length(lm5)
   N = linspace(20, maxturns5(i), maxturns5(i)-20);
   % see pg. 10
   I = (H * lm5(i))./(0.4*pi*N);
   % see pg. 2
   L = (Al5(i) * N.^2) * (10^(-9));
```

```
    plot(L,I,core5(i,:))
    hold on
end
title('Starting at 20 turns to max single layer turns at 28 awg')
xlabel(' Nominal Inductance [H]')
ylabel(' I [A] of %80 permeability')

gset output "core5.ps"
gset terminal postscript
gset output "/dev/null"
gset terminal x11

hold off
figure
for i = 1:length(lm6)
   N = linspace(20, maxturns6(i), maxturns6(i)-20);
   % see pg. 10
   I = (H * lm6(i))./(0.4*pi*N);
   % see pg. 2
   L = (Al6(i) * N.^2) * (10^(-9));
   plot(L,I,core6(i,:))
   hold on
end
title('Starting at 20 turns to max single layer turns at 28 awg')
xlabel(' Nominal Inductance [H]')
ylabel(' I [A] of %80 permeability')

gset output "core6.ps"
gset terminal postscript
gset output "/dev/null"
gset terminal x11

hold off
figure
for i = 1:length(lm7)
   N = linspace(20, maxturns7(i), maxturns7(i)-20);
   % see pg. 10
   I = (H * lm7(i))./(0.4*pi*N);
   % see pg. 2
   L = (Al7(i) * N.^2) * (10^(-9));
   plot(L,I,core7(i,:))
   hold on
end
title('Starting at 20 turns to max single layer turns at 28 awg')
xlabel(' Nominal Inductance [H]')
ylabel(' I [A] of %80 permeability')

gset output "core7.ps"
gset terminal postscript
gset output "/dev/null"
gset terminal x11

hold off
figure
```

```
for i = 1:length(lm8)
   N = linspace(20, maxturns8(i), maxturns8(i)-20);
   % see pg. 10
   I = (H * lm8(i))./(0.4*pi*N);
   % see pg. 2
   L = (Al8(i) * N.^2) * (10^(-9));
   plot(L,I,core8(i,:))
   hold on
end
title('Starting␣at␣20␣turns␣to␣max␣single␣layer␣turns␣at␣28␣awg')
xlabel('␣Nominal␣Inductance␣[H]')
ylabel('␣I␣[A]␣of␣%80␣permeability')

gset output "core8.ps"
gset terminal postscript
gset output "/dev/null"
gset terminal x11

hold off
figure
for i = 1:length(lm9)
   N = linspace(20, maxturns9(i), maxturns9(i)-20);
   % see pg. 10
   I = (H52 * lm9(i))./(0.4*pi*N);
   % see pg. 2
   L = (Al9(i) * N.^2) * (10^(-9));
   plot(L,I,core9(i,:))
   hold on
end
title('Starting␣at␣20␣turns␣to␣max␣single␣layer␣turns␣at␣28␣awg')
xlabel('␣Nominal␣Inductance␣[H]')
ylabel('␣I␣[A]␣of␣%80␣permeability')

gset output "core9.ps"
gset terminal postscript
gset output "/dev/null"
gset terminal x11

hold off
figure
for i = 1:length(lm10)
   N = linspace(20, maxturns10(i), maxturns10(i)-20);
   % see pg. 10
   I = (H52 * lm10(i))./(0.4*pi*N);
   % see pg. 2
   L = (Al10(i) * N.^2) * (10^(-9));
   plot(L,I,core10(i,:))
   hold on
end
title('Starting␣at␣20␣turns')
xlabel('␣Nominal␣Inductance␣[H]')
ylabel('␣I␣[A]␣of␣%80␣permeability')

gset output "core10.ps"
```

```
gset terminal postscript
gset output "/dev/null"
gset terminal x11
```

Appendix D

AC Light Dimmer

This appendix presents a portion of Ken Schrock's final 6.131 project. Ken built the AC light dimmer shown in Figure D.1. This circuit, like most AC dimmers, uses phase-control to modulate the power delivered to a load. Phase-control is similar to PWM, in that only a portion of the full AC waveform is delivered to the load.

This circuit uses a TRIAC in series with the light bulb. A TRIAC is turned on with a pulse of current at its gate. It stays ON so long as the voltage across it is non-zero. This circuit detects a zero-crossing in the utility, and then pulses the gate after some time delay. The TRIAC will turn ON, and stay ON until the next zero-crossing, thereby modulating the power delivered to the load. Changing the delay after the zero-crossing will change how much of the AC waveform "gets through" to the bulb: longer delays will result in less power.

This circuit uses a LM311 as a zero-crossing detector. An attenuated version of the utility is capacitively coupled on to a 2.5 V reference, and then compared with another 2.5 V reference. This creates a square-wave with rising and falling edges at the zero-crossings. This square-wave is passed into a one-shot, the 74LS122, which creates an adjustable delay before signaling the TRIAC to turn ON. A rising-edge on the output of the 74LS122 triggers another one-shot, the 74LS123, to fire. This one-shot has a programed pulse-width that injects current into the gate of the TRIAC, turning it ON.

Interestingly enough, although this circuit is functionally a half-wave phase controller, since the 74LS122 is only sensitive to the rising edge, the unstable performance of the LM311 during the zero-crossings produces many rising and falling edges on the output. Thus, in practice, it often functions as a full-wave phase controlled dimmer.

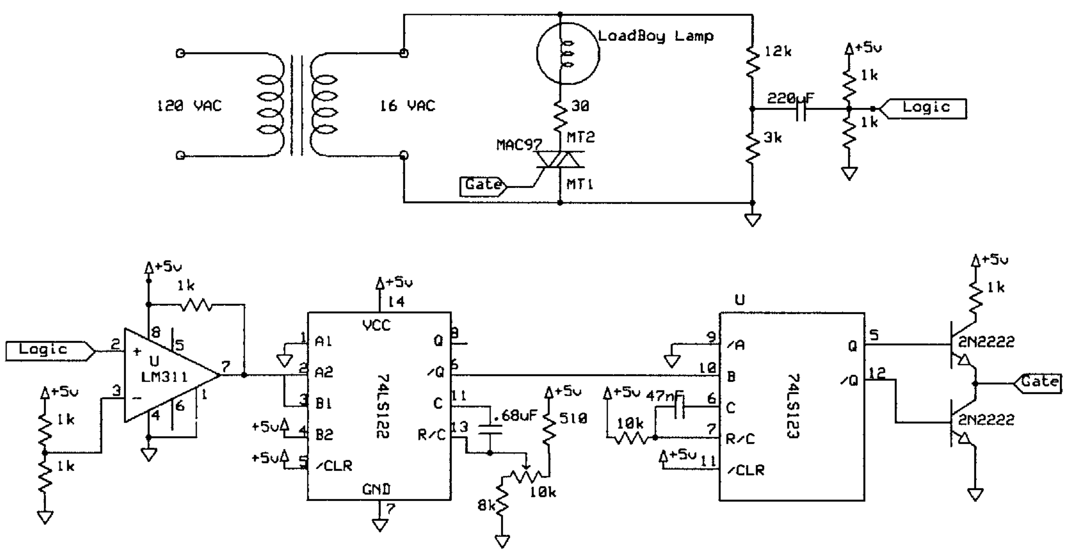

Figure D.1: A digital, phase-controlled light dimmer.

Bibliography

[1] Eta Kappa Nu MIT Chapter. *The Underground Guide.* January 2005.

[2] Robert Warren Erickson. *Fundamentals of Power Electronics.* Kluwer Academic Publishers, 2001.

[3] Steven B. Leeb. *6.131: Lab 1, Linear versus Switching Power Amplifiers.* 2004.

[4] Steven B. Leeb. *6.131: Lab 2, Canonical Cell Switching Converters.* 2004.

[5] Steven B. Leeb. *6.131: Lab 3, AC Generation, Control, and Transformers.* 2004.

[6] Steven B. Leeb. *6.131: Lab 4, Motors and Drives.* 2004.

[7] Ned Mohan, Tore M. Undeland, and William P. Robbins. *Power Electronics: Converters, Applications, and Design.* John Wiley and Sons, Inc., 1995.

[8] Ariel Rodriguez. *Advanced Undergraduate Project: Drive Circuit Design for Power Electronics.* May 2005.

[9] Ken Schrock. *6.131 Final Project Report.* 2004.

[10] Eric Tung. *Master of Engineering Thesis.* Pending.

[11] John F. Waymouth. *Electric discharge lamps.* M.I.T. Press, 1971.

[12] Candace N. Wilson. *6.131 Final Project Report.* 2004.

[13] Candace N Wilson. *Advanced Undergraduate Project: Approximating Core Loss in the Fluorescent Lamp.* May 2005.